DIMENSIONLESS PARAMETERS IMPORTANT TO THE PREDICTION OF VORTEX-INDUCED VIBRATION OF LONG, FLEXIBLE CYLINDERS IN OCEAN CURRENTS

J. Kim Vandiver

MITSG 91-13

Sea Grant College Program
Massachusetts Institute of Technology
Cambridge, Massachusetts 02139

Grant No: NA86AA-D-SG089

Project No: RO-31

DIMENSIONLESS PARAMETERS IMPORTANT TO THE PREDICTION OF VORTEX-INDUCED VIBRATION OF LONG, FLEXIBLE CYLINDERS IN OCEAN CURRENTS

By

Prof. J. Kim Vandiver

Massachusetts Institute of Technology
Cambridge, Massachusetts

ABSTRACT

Case studies drawn from fifteen years of field and laboratory experiments are used to demonstrate and explain why the flow-induced vibration of long cylinders in ocean currents varies from single mode lockin to broad band random vibration. It is shown that the range of observed behavior is predictable with careful consideration of a few dimensionless parameters. New interpretations are given to the significance of familiar parameters such as mass ratio and reduced damping. In addition the fractional variation in flow velocity over the length of the cylinder and the number of natural frequencies within the bandwidth of the vortex shedding frequencies are shown to be of considerable importance.

When consideration of the above parameters reveals that multiple mode response without lock-in is likely to occur, then hydrodynamic damping is revealed to have a powerful influence on dynamic response, and the simple product of the total damping ratio and the mode number allows one to anticipate the whole range of response behavior, from the wave propagation properties of infinite length cables to the standing wave features of short cylinders.

NOMENCLATURE

$y(x,t)$	= cross flow response displacement
m	= structural mass per unit length not including added mass
T	= tension
x	= response measurement point
k	= wave number = w/C
ω	= vibration frequency, (rad/s)
ω_s	= local mean vortex shedding frequency
C	= phase velocity of waves in the cable $(=\sqrt{T/m})$
L	= the cylinder length

s.g.	= specific gravity
ρ_f	= fluid density
ρ_w	= water density
D	= cylinder diameter
S_t	= Strouhal number
V(x)	= flow velocity at x
V_R	= reduced velocity
V_{max}	= peak velocity in a linear shear
V_{rms}	= turbulence standard deviation
N_s	= the number of modes within the shear bandwidth
ω_n	= natural frequency of mode n
ω_{max}	= natural frequency closest to the peak shedding frequency
ζ_n	= damping ratio for mode n
$\zeta_{h,n}$	= hydrodynamic part of modal damping ratio
$\zeta_{s,n}$	= structural part of modal damping ratio
B	= velocity squared damping coefficient

INTRODUCTION

The vortex-induced vibration of a long flexible cylinder such as a mooring cable or a deep water petroleum production riser, depends on many dimensionless parameters acting in concert. The prediction of the vibration requires that one weigh the relative influence of each parameter and estimate the probable outcome. A sequential approach is used in this paper, beginning with the determination of whether or not lock-in is possible. The most important parameters in this determination are shown to be: the shear fraction, $\Delta V/V_{MAX}$, and the number of resonant natural modes within the shear excitation bandwidth, N_s. Also important are the reduced damping, S_c, mass ratio, μ, and turbulence intensity. When it is determined that lock-in is likely, then it is possible to turn to a large established literature to make precise estimates of response amplitudes [e.g. Griffin & Ramberg, 4].

When lock-in is not the predicted response, there are three principal causes: i) The reduced damping is sufficiently large that no significant motion results. ii) The vortex shedding frequency does not correspond to any natural frequency. iii) The excitation bandwidth includes the natural frequencies of more than one mode, resulting in a multi-moded response with random vibration characteristics.

Of the three reasons the third, multi-moded behavior, is the least well understood and is of considerable practical importance. This subject is examined in detail in this paper. In this case $\Delta V/V_{MAX}$ and N_s are important parameters, in that they are reliable indicators of multiple mode nonlock-in response. When multiple mode nonlock-in response is the prediction then another parameter is useful in characterizing the expected dynamic properties of the cylinder. This parameter is $n\zeta_n$, the product of the mode number and the total damping ratio for the responding mode. The total damping ratio, includes the hydrodynamic contribution. This parameter is recognized in the field of mechanical vibration by several names. It can be derived by considering the attenuation of a wave travelling the length of the cylinder or it can be derived by calculating the ratio of the half power bandwidth of mode n to the separation in frequency between modes. Thus it is a measure of what is known as modal overlap. Regardless of the way one derives or defines this parameter, it is useful in anticipating those cylinders, which will behave as if of infinite length, versus those which exhibit standing waves and mode shapes.

EVALUATING CONDITIONS FAVORABLE TO LOCK-IN

By the mid 1970's a great deal of laboratory scale research had been completed by many investigators on fixed and moving cylinders in fluid flows. Concepts such as lock-in, correlation length, and drag coefficient dependence on response amplitude were quite well developed. Missing at the time were systematic experiments on long flexible cylinders which could rationally extend the observations made in laboratory scale tests to field applications of much larger scale.

The Early Castine Experiments

In the summers of 1975 and 1976, the author, with the sponsorship of the Office of Naval Research, conducted experiments in a tidal flow at Castine, Maine. Most of the cylinders tested were synthetic fiber, or wire cables, 75 feet in length with diameters

varying from 1/4 to 5/8ths of an inch. Flow velocity was quite spatially uniform and varied with time from 1/2 to 2 1/2 feet per second. The typical vibration response was single mode lock-in with response amplitudes of ±1 diameter at the antinodes. At certain flow velocities there were occurrences of a lower amplitude random vibration response which was named nonlock-in behavior, Vandiver & Mazel, 1976 [18]. The Reynolds number range for these tests was from 800 to 10,000 and the reduced damping was very low. The observed response was rather insensitive to variations in Reynold's number as well as to large amounts of surface roughness, due typically to the cable braid or the helical lays of rope.

An initially inexplicable, but ultimately significant, event occurred. On one occasion a plastic jacketed wire rope 0.280 inch in diameter and 900 feet in length was stretched across the tidal basin from two points of land. The submerged portion of the cable was approximately 500 feet long and was exposed to flow which varied approximately 20% along the length. In spite of the shear lock-in occurred at approximately the 50th mode. Response amplitudes of ±1/2 to ±1 diameter were observed. This established that lock-in is possible at very high mode numbers in the presence of a mild shear.

Castine, 1981

A much more ambitious experiment, sponsored by ONR, the U.S. Geological Survey, and a consortium of industry sponsors, was conducted in the summer of 1981 at the same site at Castine, Maine. The experiment lasted 6 weeks and involved 8 people in the field with the research vessel Edgerton from the MIT Sea Grant Program. The experimental setup is shown in Figure 1.

Two test cylinders were used in the experiments. The first was a cable 75 feet in length, 1¼ inches in diameter, containing 7 biaxial pairs of accelerometers. In the experiments, tension, acceleration, current and mean drag coefficient were measured. This cable was also pulled inside of a 1.625 in. diameter steel pipe, which was then used as the second test cylinder. The pipe was

selected to provide a cylinder with a significantly different mass ratio and a non-negligible bending rigidity. Properties of the test cylinders are given in Table 1.

The primary objectives of this field experiment were to (1) measure mean drag coefficients under field conditions and compare them to the very high values observed under laboratory conditions, (2) determine the differences in behavior of cables and pipes with significant differences in bending stiffness and mass ratio, and (3) test cable behavior with attached lumped masses. The behavior with lumped masses is reported in Griffin & Vandiver, 1984 [6].

TABLE 1 - MECHANICAL PROPERTIES AND DIMENSIONS OF TEST CYLINDERS

Cable Specifications

Length:	75.0 ± 0.1 feet
Diameter:	1.25 ± 0.02 inches
Weight per foot in air:	0.7704 pounds per foot
Specific Gravity:	1.408

Pipe Specifications

Length:	75.0 ± 0.02 feet
Outside diameter:	1.631 ± 0.003 inches
Inside diameter:	1.493 ± 0.003 inches
Weight per foot in air including weight of the internal cable:	2.001 pounds per foot
Weight per foot including cable and trapped water:	2.236 pounds per foot
Specific gravity of pipe with cable and trapped water:	2.40
Measured bending stiffness, EI:	$(3.016 \pm 0.05) \times 10^6$ pound inches^2

The field measurements of drag coefficients are presented in Figures 2 and 3 from Vandiver, 1983 [13]. Figure 2 shows the drag coefficient for the pipe measured over a period of 2 1/2 hours. The data is moving average data. Every data point in the plot is a sliding average of 8.55 seconds of observation. Also shown in the figure are the moving averages of the flow velocity and the rms vibration amplitudes observed in the cross flow vibration direction and the in-line vibration direction at one location on the cylinder. The location was at L/6, or 1/6th of the length from one end of the cylinder.

In Figure 2 for the pipe the data reveals periods or plateaus of high drag coefficient adjacent to periods of relatively low drag coefficient. The plateaus are at times of lock-in with individual modes which are indicated in the figure; for example, 2nd and 3rd mode. At these times the natural frequency of the cylinder for the mode indicated, coincided with the vortex shedding frequency. The valleys in drag coefficient occurred at times when the flow velocity was such that wake synchronization could not occur. At these times vibration still occurred but with lower rms amplitudes and with broader band random vibration characteristics, than occurred during single mode lock-in. Under lock-in conditions the drag coefficients were greater than two times the value of a similar non-moving, rigid cylinder at the same Reynolds number.

The reported in-line and cross flow rms response measurements shown in the figures are plotted for only one location, L/6. The response amplitude at this location is influenced by mode shape. For example this location would show zero response for vibration in the sixth mode, and would show maximum antinode response for the third mode. One must not, therefore, attempt to draw quantitative conclusions about response amplitude from these rms plots without taking mode shapes into consideration. Modal response amplitudes have been evaluated for these experiments by Vandiver and Jong, 1987 [17].

Figure 3 is also a 2 1/2 hour record, but for the cable. Again very high drag coefficients are observed. However, there is

one remarkable difference between the cable data and the data shown for the pipe in Figure 2. There are no obvious plateaus and valleys in the drag coefficient. There are no clear demarcations between periods of lock-in and nonlock-in behavior. That difference in mass ratio between the pipe and the cable was the cause of the difference in response, did not become clear until a few years later. This is discussed in the next section.

The drag coefficient data deserve further explanation. They are least accurate at low flow speeds. This is due to absolute errors in zeroing the load cell under field conditions. These absolute errors lead to large percentage errors at low flow speeds when the drag force is small. For the cable data, the large increase in measured drag coefficient at the end of the run is due to such an offset error. The error bounds are given with the figure titles.

The Importance of Mass Ratio

The mass ratio is $m/\rho_f D^2$. It is $\pi/4$ times the ratio of the mass per unit length of the cylinder (m) to the mass per unit length of the displaced fluid, $(\pi\rho_f D^2/4)$. Some authors include the added mass when reporting the mass per unit length. This should be avoided because the added mass is not constant, as will be discussed below.

Figure 4, reproduced from Chung, 1987 [2], shows data from a variety of sources. Response amplitude is plotted versus reduced velocity for a variety of cylinders with different mass ratios. The reduced velocity, V_R, in this figure is based on the in air natural frequency, which to sufficient accuracy is the same as the in vacuo value. In other words an added mass coefficient of zero has been used. The data for a mass ratio of 0.78 (specific gravity = 1.0) is for first mode vibration of a neutrally buoyant aluminum tube, 120 mm diameter, 9.93 m long, immersed in water; from Steve Koch, 1985 [21].

The remarkable conclusion that one can draw from this figure is that low mass ratio cylinders have a much broader lock-in range

than high mass ratio ones, when the reduced velocity is computed using the measured flow speed and the in air natural frequency, not the observed vibration frequency. This property is the key to understanding the difference between the response characteristics of the pipe and the cable in the 1981 Castine experiments.

Large amplitude, self-excited, lock-in occurs, if and only if, there is a synchronization of the periodic formation of vortices in the wake and resonant motion of the cylinder. The range of frequencies which permit this synchronization is governed by two factors. One is the response bandwidth of the resonant peak of the oscillator, which is given approximately by twice the damping ratio, multiplied by the natural frequency: $2\zeta_n\omega_n$. For example, a resonant mode with one per cent damping will have a resonant bandwidth of approximately two per cent of the natural frequency. For a fixed natural frequency this is much too small to explain the wide lock-in bands exhibited in Figure 4. The second factor is the tolerance of the wake synchronization process to variations in reduced velocity resulting from changes in flow speed. Hereafter, this will be referred to as the lock-in bandwidth of the wake.

Driven cylinder experiments have shown that for a fixed vibration frequency, and favorable cross flow vibration amplitudes, the range of flow velocity, and therefore reduced velocity, that permits wake synchronization is narrow. The typical lock-in bandwidth of the wake, expressed in reduced velocity terms is approximately 5.0 to 6.5, or about a 25% variation. Of course the precise limits of this range also depend on Reynold's number, turbulence intensity, and roughness. Taking all of these into consideration, however, the conclusion is the same; the lock-in bandwidth of the wake is much narrower than the lock-in range exhibited by low mass ratio cylinders such as those shown in Figure 4.

Therefore, the only remaining explanation of the wide resonant lock-in range shown in the figure for some cylinders is that the cylinder resonant response frequency is not constant, but must be increasing, as the flow velocity increases. Close inspection of response frequency data for low mass ratio cylinders, reveals that

over the lock-in range the response frequency increases with the flow velocity. This effect is most pronounced for the lowest mass ratio cylinders.

The rise in the resonant, response frequency with flow speed is due to the variation in the added mass coefficient over the lock-in range. There is driven cylinder data by Sarpkaya, 1977[9], to support this hypothesis. His data reveals that at an amplitude to diameter ratio of 0.5 the added mass coefficient decreases sharply from values of 5.5 to -.8, as the reduced velocity varys from 2.5 to approximately 5.5. The added mass coefficient then rises slowly to about -0.5 as the reduced velocity increases to the limits of the data at 8.0. This phenomenon is similar for a wide range of vibration amplitudes. The consequence of importance in the context of the lock-in bandwidth is that, if the added mass decreases with increasing reduced velocity then the natural frequency of the cylinder will increase. This allows the lock-in region to persist to higher values of flow speed.

This effect is less for high mass ratio cylinders, because the added mass is a lower percentage of the total mass per unit length. Equation (1) gives an expression for the natural frequencies of a submerged beam or cable with pinned ends and under constant tension showing the effect of the added mass coefficient.

$$\omega_{n,fluid} = [(n\pi/L)^2T + (n\pi/L)^4EI]^{\frac{1}{2}}[\rho_f D^2(\mu+\pi C_a/4]^{-\frac{1}{2}} \qquad (1)$$

where:

L	=	length,
T	=	tension,
μ	=	mass ratio = $m/\rho_f D^2$
m	=	mass per unit length without added mass
C_a	=	added mass coefficient
E	=	Young's modulus
I	=	area moment of inertia of the beam
n	=	mode number
ρ_f	=	fluid density

When the added mass coefficient is zero the above equation yields the in air natural frequency, $\omega_{n,air}$. The above expression

for the submerged natural frequencies may also be expressed as the product of the in air natural frequencies and a simple function of the added mass coefficient, as follows.

$$\omega_{n,fluid} = \omega_{n,air} \times [1+(\pi C_a/4\mu)]^{-1} \qquad (2)$$

This equation may be solved for the added mass coefficient, C_a. By substituting the values of experimentally observed vibration frequencies in this expression, one may calculate the effective added mass coefficient. This was the objective of a set of experiments recently conducted by T.Y. Chung, he measured the self-excited cross flow response amplitude and frequency for five flexible cylinders in water with mass ratios varying from 1.6 to 6.1 [3]. The experiment was conducted in the recirculating cavitation tunnel of the Korea Research Institute of Ships and Ocean Engineering. The cylinders were 6.0 mm in diameter and 0.6 m long. His response amplitude versus reduced velocity data were consistent, as expected, with the behavior shown in Figure 4: that is lower mass ratio cylinders have broader lock-in bandwidths than high mass ratio ones. He used the observed vibration frequency data to calculate effective added mass coefficients. These are plotted versus reduced velocity in Figure 5. Also plotted on the figure are the added mass curves from Sarpkaya[9] for amplitude to diameter ratios of 0.5 and 0.75. The amplitude of vibration of the experimental cylinders was in the form of the half sine wave mode shape of the first mode of vibration, and therefore, varied from 0.0 at the ends to a maximum at the midspan. The midspan amplitude varied with reduced velocity in the lock-in range from 0.2 to 1.3 diameters. Since Sarpkaya's data show that the added mass is sensitive to amplitude then Chung's results reflect an effective aggregate added mass, which represents a form of spatial average of the local added mass. Furthermore for each reduced velocity the peak amplitude of Chung's test cylinders was different. Therefore, it is not possible to make a one to one comparison between the Sarpkaya curves and the calculated effective added mass coeffi-

cients. Nonetheless the similarity between Chung's effective added mass coefficients and Sarpkaya's data supports the theory that variation in added mass allows the natural frequency to rise with flow speed.

The effect of mass ratio, as presented above must be taken into account when predicting the likelihood of lock-in response of flexible cylinders in uniform flows. For example, tensioned cables with negligible bending stiffness have uniformly spaced natural frequencies. For each natural frequency there is a range of flow speeds which may permit lock-in. The width of this range is governed by the mass ratio. Low mass ratio will result in large variation in natural frequency and thus cause the overlap of the lock-in range of each natural mode with the neighboring modes. This was the case with the cable tested at Castine in 1981, and described earlier. The cable had a specific gravity of 1.408 (μ=1.106). Judging from the data in Figure 4, such a cable would be able to lock-in over a range of reduced velocities from approximately 4 to 8. This corresponds to a doubling in flow velocity. Thus the lock-in range of the first mode of the cable extended to the range of the second mode which had an in air natural frequency twice that of the first mode. Similarly the second, third and higher modes had overlapping lock-in regions. The cable tested at Castine was able to lock-in at all flow speeds, with typical response amplitudes of ±1 diameter at the antinodes.

Since the natural frequencies are uniformly spaced for a constant tension cable, the overlap of the modes becomes greater at higher mode numbers. At the tenth mode, a lock-in bandwidth of less than ±10% would overlap the lock-in bands of the 9th and 11th modes. Thus, all constant tension cables, independent of mass ratio, will have overlapping lock-in ranges for mode numbers exceeding the tenth mode and many cables, with low mass ratio will have overlapping lock-in ranges at much lower mode numbers.

Beams under tension behave differently. At low mode numbers, tension effects may be dominant, and the natural frequencies may be similar to those of cables, as one can deduce from Equation (1).

At higher mode numbers, the bending effects become important. When the bending effects are dominant the natural frequencies increase as n^2 and the separation between natural frequencies increases in proportion to 2n. Thus for beams under tension, if the lock-in regions do not overlap for low modal frequencies, they probably wan't at high mode numbers either.

The pipe tested at Castine experienced lock-in at its first four natural frequencies, as dictated by the flow speed. The lock-in regions did not overlap, and as flow speed increased the pipe exhibited clearly defined ranges of lock-in and nonlock-in behavior. The lock-in ranges did not overlap. This was not because the pipe had greater separation between natural frequencies than did the cable. In fact the first four excited modes for both the pipe and cable had quite similar in air natural frequencies. For example, the first five natural frequencies for the cable at 792 pounds tension were 1.20, 2.39, 3.58, 4.79 and 6.08 Hz. For the pipe at 1000 pounds tension the first five natural frequencies were 0.86, 1.77, 2.86, 4.26 and 5.73 Hz. The clear lack in the overlap of the lock-in regions for the pipe was primarily due to difference in mass ratio. The specific gravity of the pipe was 2.4 (μ=1.89), and it was, therefore, less sensitive to changes in added mass than was the cable, which had a specific gravity of 1.41. As a consequence the pipe had a narrower lock-in range than the cable, permitting the existence of nonlock-in regions between lock-in ones.

In-line response: As biaxial accelerometers were used it was possible to observe both the cross flow and in-line response of the cable and pipe. It was discovered that the in-line response was highly correlated to the cross flow, especially under lock-in conditions. The correlation was non-linear and could be approximated by a square law model. This correlation is discussed in reference [17].

Reynold's Number Dependence

The Reynold's number range encountered in the tests at Castine was from zero to 10,000. Vibration was observed above approximate-

ly 300. From 300 to 10,000 the vibration behavior seemed to have little Reynold's number dependence. Cylinder motion appears to be more important than Reynold's number in determining lock-in characteristics. Further evidence of this insensivity of flow-induced vibration to Reynold's number may be found in numerous reports of the large amplitude vibration of drilling risers and pilings; for example Griffin & Ramberg, 1982 [4].

The Tolerance of Lock-in to Small Amounts of Shear

The 900 foot long wire rope test: When two or more modes are within the lock-in range, one may dominate. The long wire rope tested in 1975 had at least ten modes potentially capable of lock-in. Somehow, one mode, approximately the fiftieth was able to dominate. This was in spite of the fact that the flow speed varied approximately 20% along the submerged portion of the cable. Lock-in was possible because a 20% variation in speed, and therefore reduced velocity, is within the tolerance of the wake to remain synchronized with a cylinder vibrating at one frequency. In this case the mode, which was, apparently, best positioned in frequency to lock-in over the entire length, dominated. As the tidal current slowly changed, the responding mode would change, interspersed with periods of random vibration, characteristic of nonlock-in behavior. The mode number was estimated by measuring the distance between vibration nodes, which were clearly visible on the portion of the cable which was not submerged.

A subtle question remains, regarding the relative importance of shear and mass ratio in determining the possibility of lock-in. Consider a low mass ratio cylinder with a reduced velocity lock-in range of 4 to 8, as shown in Figure 4. If this cylinder were exposed to a shear flow profile which doubled in speed from one end to the other, such that the reduced velocity, based on the in air natural frequency, varied from 4 to 8, would the cable be able to lock-in over the entire length? The answer is emphatically no. Although the added mass coefficient may vary along the length, the aggregate added mass on the cable results in a single resonant

frequency for each mode and shear profile. At any specific frequency, the lock-in tolerance bandwidth of the wake is on the order of 20%, as previously revealed in numerous forced cylinder oscillation tests. Therefore, the wake synchronization regions of cylinders in sheared flows is restricted to zones over which the velocity varies by approximately 20%.

Is it then possible for a long cylinder in a sheared flow to be divided up into zones of 20% current variation, with each zone exhibiting lock-in with a different mode at a different natural frequency? Again the answer is no, because multiple frequency components in the response are sufficient to prevent lock-in, as discussed in the next section. It is not possible for more than one mode at a time to synchronize with the wake.

The Effect of Irregular Cylinder Motion on Lock-in

In the late 70s, a likely lock-in prevention mechanism, which had not been previously studied, was irregular motion of the cylinder. A laboratory experiment was conducted to test the hypothesis that the introduction of a small amount of random cylinder motion, while maintaining a mean frequency most favorable to lock-in, could in fact prevent wake synchronization and, hence, lock-in from occurring. A set of driven cylinder experiments were conducted on a rigid cylinder 0.5 inch in diameter and 20 inches long in the MIT Ocean Engineering Department's circulating water tunnel. The cylinder was driven in cross flow vibration by an electromagnetic shaker. The cylinder vibration amplitude and spectral shape were varied in a controlled fashion. The spectral shape varied from sinusoidal to random with narrow to broad band characteristics. Flow velocity, hence reduced velocity, was systematically varied. Cylinder motion and drag force were measured. Wake velocity components were measured with a laser doppler anemometer.

Under sinusoidal lock-in conditions near unity coherence was observed between wake velocity measurements and cylinder motion. However, when the cylinder motion was changed to a narrow band random process with a center frequency the same as would usually

result in lock-in, the coherence between cylinder motion and wake velocity dropped [Figures 6 and 7]. Broad band cylinder vibration reduced the coherence to near zero. The mean drag coefficient was also measured. The disruption in the lock-in process by random motions of the cylinder caused 50% reductions in drag coefficient, Shargel & Vandiver, 1982 [11].

An important conclusion to be drawn from these experiments is that lock-in is a rather fragile phenomenon which can be reduced or prevented by vibration frequency components not at the lock-in frequency. An application of considerable significance is the response prediction problem in sheared flow. Vibration, generated at one location and with a particular frequency, may propagate to another, where the local flow velocity, hence, lock-in frequency range, is different. The existence of the foreign generated frequency components in the local vibration response, may be sufficient to prevent lock-in.

The maximum shear which can be tolerated and yet allow a cylinder to respond in a locked-in fashion is not known. It is probably very dependent on whether or not a second resonant frequency is included in the bandwidth of shedding frequencies which could be created by the given profile. If only one resonance is possible, then lock-in is possible, even with a rather large shear. The likely behavior would be that the cylinder would lock-in over as much of the length as allowed by the lock-in bandwidth of the wake, which has been indicated to be on the order of 20%. The remainder of the cylinder would be in an unsynchronized region providing additional damping. An example of such a phenomena is the case of vertical pilings exposed to tidal flow, with large variations in the flow profile. Without a second resonant mode, simultaneously excited by the shear, there are insufficient foreign frequency components in the response to disrupt the lock-in behavior in the region that is driving the cylinder. For most cases the additional damping contributed by the nonlock-in regions is not sufficient to prevent lock-in. Damping is important, however, and is discussed next.

The Reduced Damping Parameter

Response amplitude prediction under lock-in conditions has long been based on a dimensionless parameter known variously as the "reduced damping", the "stability parameter", or simply the "response parameter". This is sometimes written as S_c or ζ/μ, and defined below; Griffin & Ramberg, 1982[4]

$$\zeta/\mu \equiv S_c \equiv 2\pi S_t^2 (2m\delta/\rho_f D^2) \qquad (3)$$

where:

$\delta = 2\pi\zeta$, the logarithmic decrement

$2\pi S_t = \omega D/V$

$\zeta = r/(2\omega m)$, the damping ratio

The last expression assumes that the damping constant per unit length, r, is uniformly distributed along the cylinder. If this is not the case, one may replace r and m in the above expression by the modal damping and modal mass constants which can be computed by the techniques of modal analysis.

The reduced damping parameter is both useful and very often misinterpreted. As this parameter increases, response decreases. From equation 6 one can see that S_c becomes large for large values of damping ratio or for small values of mass ratio. The common erroneous conclusion is that low density cables, hence ones with small mass ratio, are likely to respond more than high density ones. In fact mass ratio has little to do with the response amplitude. When one replaces the Strouhal number, the damping ratio, and the mass ratio, in equation 3 with the definitions given, the following expression for S_c results. It is independent of cylinder mass.

$$S_c = r\omega/(\rho_f V^2) \qquad (4)$$

S_c is essentially the ratio of dissipative forces on the cable to hydrodynamic exciting forces. It is a statement of dynamic

equilibrium between the average power injected into the cable by the fluid through lift forces and the power dissipated by damping. Such an equilibrium exists for all cases including shears. One must however properly account for the hydrodynamic and structural sources of damping in each case, and must also properly account for the fluid excitation regions on the structure. Vandiver, 1985 [14], addresses this topic in some detail.

If one wishes to use the reduced damping parameter to estimate response amplitude under lock-in conditions, then one must measure or estimate the correct damping. If the cylinder is expected to lock-in over its entire length, then the appropriate damping is the damping which one would measure in an in vacuo transient decay test. This is often called the structural damping and when expressed as a fraction of the critical damping ratio is written as ζ_s. For cylinders immersed in water, it is sufficiently accurate to use the structural damping ratio measured in air.

At Castine the in air measured damping ratios for the 2nd, 3rd, and 4th modes of the cable were 0.002 ±0.0005 at a vibration amplitude of one diameter. For the pipe the damping ratios for the same modes were 0.002, 0.0015, and 0.001, with an accuracy of ±0.0005. Thus for the pipe and cable at low mode numbers the reduced damping did not exceed 0.002. Thus on the basis of much empirical data, one would expect that the lock-in response amplitude for these cylinders would be approximately ±1 diameter at the antinodes, as was observed.

There are times of lock-in when one must include some hydrodynamic damping in the reduced damping calculation. These times correspond to lock-in conditions that do not include the entire length of the structure. An example might be a layered flow, in which a uniform flow exists over a portion of a cable, and the remainder of the cable is immersed in non-moving fluid. Hydrodynamic damping must be included for the portion of the cable in the non-moving fluid. Though such an example is admittedly contrived, such conditions exist in experimental facilities equipped with flow channels which pass over deep pits, used for testing long objects.

CONDITIONS FAVORABLE TO MULTIPLE MODE NONLOCK-IN BEHAVIOR

Sheared Flow Experiments in the Arctic and St. Croix

In 1982 a controversy developed within U.S. Navy circles regarding the correct drag coefficient to use in the design of very long mooring cables exposed to realistic, sheared, ocean currents. Was it necessary as a design precaution to use drag coefficients measured under lock-in conditions or were the reduced drag coefficients seen in the presence of random vibration more appropriate? In a strongly sheared current, would lock-in ever occur?

In 1983 two experiments were conducted on long, small diameter cables with the purpose of resolving the controversy. A shakedown experiment was first conducted on a vertical cable hung through the ice in the Arctic. Six months later a much more elaborate experiment was conducted from a United States Navy barge at St. Croix in the U.S. Virgin Islands. A braided Kevlar cable 0.16 inch in diameter was hung vertically at lengths up to 2000 feet under tensions of approximately 20 pounds. A 0.094 inch Kevlar cable was also tested at lengths up to 9000 feet. The current varied from a maximum of about 1.1 ft/s at the surface to a minimum of approximately 0.1 ft/s at depth, with substantial variations in between. Lock-in never occurred. Broad band random vibration did occur as can be seen in Figures 8 and 9. Accelerometer measurements, made as little as 275 feet apart, were uncorrelated as shown in Figure 10. The cables responded to the vortex shedding as if they were of infinite length [Kim, Vandiver & Holler, 1985,7].

The uncorrelated response between the two locations could only be explained by invoking a total effective damping on the cable of 1.0 to 1.5% of critical, ten times the value of the measured structural damping. This observation was the first clear evidence that an important property of multi-moded, nonlock-in response was a large hydrodynamic damping component. This topic is addressed more fully later in the paper.

Drag coefficients, deduced from top tension and angle measurements, were found to be approximately 1.5. The corresponding rigid

cylinder value in the Reynolds number range of 200 to 2000 is about 1.2. High drag coefficients, typical of lock-in conditions, were never observed. Rms response amplitudes of 1/4 to 1/2 a diameter were observed. For these particular cables and shear conditions, the controversy was resolved. To generalize the observations requires the specification of appropriate dimensionless parameters, which can be used to predict the variations of response: from single mode lock-in, seen in the Castine experiments, to the broad band infinite cable behavior characteristic of the St. Croix experiments.

Useful Dimensionless Parameters

In the author's opinion the two most useful parameters for predicting whether or not lock-in will occur under sheared flow conditions are the number of natural modes contained in the bandwidth of vortex shedding frequencies, hereafter referred to as N_s, and the dimensionless shear fraction, $\Delta V/V_{MAX}$. Other parameters may also be influential, though generally of secondary importance. For example, in some unusual circumstances the turbulence intensity may be large enough to prevent lock-in. Unusually high structural damping would also reduce the probability of lock-in under sheared flow conditions.

When it has been established that lock-in is not likely to occur and that the response will be dominated by the simultaneous contributions of many modes, then further consideration must be given to the role of hydrodynamic damping, because it is important in determining the nonlock-in dynamic response characteristics of the cylinder. At times wave propagation effects, characteristic of an infinite cylinder, are dominant. Under other conditions standing waves, characteristic of short resonant systems, are dominant. The parameter $n\zeta_n$ will prove to be the key to anticipating such behavior.

Thus, one determines if the necessary conditions are met to create multiple mode nonlock-in response, by evaluating the shear fraction and the number of excited modes. If the necessary condi-

tions are met, one is then able to predict the dynamic characteristics of the cylinder, by evaluating the product of the damping(including hydrodynamic contributions) and the mode number, yielding $n\zeta_n$.

Shear fraction and the Number of Excited Modes

It has previously been discussed that lock-in is most likely to occur, when the frequency bandwidth of the lift forces includes only one system natural frequency. The excitation bandwidth is strongly influenced by the severity of the shear, because of the relationship between flow velocity and vortex shedding frequency. In this paper this excitation bandwidth is deduced primarily from the shear fraction, $\Delta V/V_{MAX}$. To a lesser extent the bandwidth is also influenced by the turbulence intensity level V_{RMS}/V_{MAX}. For a given excitation bandwidth, the number of modes likely to be included in the band is governed by the modal density of the natural frequencies of the cylinder. The spacing between natural frequencies depends primarily upon the mechanical properties of the system such as mass per unit length, stiffness, tension, and length. For example, the modal density of a constant tension cable is $1/f_1$ modes per Hz., or $1/\omega_1$ modes per(rad/s), where f_1 is the first mode natural frequency of a taught cable.

One measure of the likelihood of lock-in is then given by the product of the excitation bandwidth and the modal density. This product is simply the number of natural frequencies contained within the excitation bandwidth, and is here defined as N_S, [7].

The excitation bandwidth, Δf(Hz), due to shear can be estimated using a reduced velocity value of approximately 5.9 and the variation in the velocity over the total length of the cylinder, ΔV, yielding.

$$\Delta f = \Delta V/V_R \cdot D \qquad (5)$$

The reduced velocity value of 5.9 is used, because it represents the average value observed under field conditions for a variety of

flexible cylinders.

For the constant tension cable N_s, the potential number of responding modes, is given by:

$$N_s = \Delta f/f_1 = \Delta V/(f_1 \cdot D \cdot V_R) = .17\Delta V/(f_1 \cdot D) \qquad (6)$$

One must consider the size of this number and the shear fraction $\Delta V/V_{MAX}$, when determining whether or not lock-in will occur. Three experimental examples are discussed here: the 950 foot long cable tested at St. Croix, the short 75 foot long cable tested at Castine, Maine in 1981, and the 900 foot long wire rope tested at Castine in 1975.

St. Croix: The velocity variation at St. Croix was approximately 1.0 ft/s, yielding a shear fraction of $\Delta V/V_{MAX} = .91$. A 91 percent variation in flow velocity is much larger than the 20 or 30 % maximum lock-in bandwidth which can be tolerated by the wake. On this evidence alone, one might suspect that lock-in might not occur. However, the number of modes potentially excited by this shear should also be estimated. The modal density, $1/f_1$, for the 0.16 inch diameter Kevlar cable at a length of 950 ft and a tension of 21 pounds was 10.6 modes per Hz. Letting $V_R = 5.9$, N_s, the number of simultaneously excited modes, is found to be 135. Lock-in was never observed. Infinite cable behavior was observed.

Castine Cable, 1981: This cable is described in detail in Table 1. At 350 pounds tension, this 75 foot long, 1¼ inch diameter cable had a modal density, $1/f_1$, of 1.0 mode/Hz. The maximum current at Castine was approximately 2.5 ft/sec with a spatial variation of approximately 6%, measured over the length of the test section. This yields a ΔV of approximately 0.15 ft/sec and a variation in shedding frequency, as computed from equation 5 of 0.24 Hz. The turbulence intensity level was also very low; less than 5%.

For this case, $N_s = 0.24$, for $V_R = 5.9$. As a consequence,

lock-in was frequently observed at Castine. It happened whenever the mean flow velocity resulted in a shedding frequency which coincided closely with a natural frequency. This happened almost all of the time for the cable due to added mass variations as discussed before.

Had the above calculation been done for the pipe tested at Castine, the result would have been almost identical, because for the modes excited at Castine the pipe had almost the same modal density as the cable. However, nonresonant, nonlock-in response did occur when the mean shedding frequency fell outside the lock-in bandwidth of any one natural frequency. Under lock-in conditions, the lift force is periodic and the excitation bandwidth is very narrow. Under nonlock-in conditions, even with very uniform flow, the lift force excitation spectral bandwidth broadens substantially, and the lift force and resulting cylinder response are best characterized as random processes.

Note that N_s approaches zero as the incoming flow becomes uniform. When N_s is less than one, the possibility to excite a single natural mode of the cable is very high and single mode lock-in is very likely. Alternatively if N_s is very large, there is little chance to have lock-in, as more than one mode is always involved in the response. For the St. Croix test N_s was greater than 100, and lock-in never occurred.

Castine, 1976: 900 Foot Wire Rope: Between the two extremes described above the prediction of the occurrence of lock-in is not so clear. The .280 inch diameter, 900 foot long wire rope, tested at Castine in 1976, is a good example. The relevant data are given in the Table 2 below. The modal density for this case was 5.24 modes/Hz (computed with $C_a = 1.0$) and the shear fraction, $\Delta V/V_{MAX}$, was 0.2. Using a reduced velocity of 5.9, equations 5 and 6 yield an estimate for N_s of 9.9 modes.

Table 2. Castine Wire Rope Test

V_{MAX}	= 1.3 ft/sec	ΔV	= .25 ft/sec
T	= 350 lbs.	L	= 900 feet
D	= .280 inches	m	= .00211 slugs/ft in air

ζ_s = .001, structural modal damping ratio

$V_{RMS}/V_{MAX} \leq .05$

In this case lock-in did frequently occur. Even though N_s, the number of potentially excited modes, was nearly 10, one mode at a time dominated. The circumstances were such that, much of the time, no factor intervened to prevent lock-in. The turbulence level was too low to interfere, and the structural damping was too low to prevent lock-in.

The shear fraction was the pivotal parameter in this case. The shear fraction of approximately 20% was within the permissible lock-in bandwidth of the wake, thus allowing lock-in to occur over the entire length of the cable. However, a review of the recorded data indicates that about half the time lock-in did not occur, suggesting that had the shear been much greater in the experiment, lock-in would have been prevented.

The Boundary Between Lock-in and Nonlock-in

At this point in time the exact upper bound on lock-in bandwidth is not known. Griffin, 1985 [5], has suggested that the lock-in bandwidth might be as large as 70% of the natural frequency. He also introduces a parameter which serves the same purpose as N_s.

Stansby, 1976 [12], has shown that lock-in can exist on short driven cylinders with shear fractions greater than 20%. His test cylinders had L/D's of 8 and 16. In his experiment the shear fraction was approximately 33%, and in one scenario lock-in occurred over the entire length. However, his results show that the extent of the lock-in region in a sheared flow on a driven cylinder

is very amplitude dependent, and is related to the formation of a single coherent vortex cell in the wake. In sheared flow the presence of vibration nodes on the cylinder and spatially varying amplitudes, suggest that such long lock-in regions will not occur on typical structures with large L/D and high mode number.

When lock-in occurs with one of the lowest modes of the structure, it may happen without wake synchronization over the entire structure. This is a very typical occurrence on cantilevers, which may exhibit very large tip deflections under lock-in conditions with the lowest frequency natural mode. Often with such cylinders there are regions which are not locked in and act as hydrodynamic damping regions. Although vortex shedding is happening in these nonlocked-in regions, the frequency of the resulting lift force does not correspond to any other system natural frequency, and the resulting small response amplitudes are not sufficient at these frequencies to disrupt the lock-in process.

For long cables and risers, which respond at higher mode numbers, nonlock-in regions generate lift forces which do coincide with other system natural frequencies, creating wide band response which will prevent pure lock-in response from occurring, even in portions of the cylinder with conditions favorable to lock-in. The example of the 900 foot long cable at Castine is a data point which marks one of the boundaries of lock-in behavior.

A Not So Useful Parameter, ß

A parameter which is conspicuously missing from the earlier discussion is the shear parameter ß, because it is not particularly useful. It is usually defined as:

$$\beta = (D/V_{REF})dV/dx$$
$$= (D/L)\cdot \Delta V/V_{REF}, \text{ for linear shears} \qquad (7)$$

where V_{REF} is variously defined in the literature. Letting it be V_{MAX} for the purposes of this discussion then for linearly varying shears

$$\beta = (D/L) \cdot \Delta V/V_{MAX} \quad (8)$$

This is just the ratio of the shear fraction, which separately has usefulness, to L/D, which has little impact, except when less than approximately 20 to 30. β can in fact be quite misleading, because the directly useful information embodied in $\Delta V/V_{MAX}$ is obscured in the division by L/D.

Neither the shear parameter nor the shear fraction give an indication as to the dynamic response of the cable. That this is so can be simply proven. Consider a cable with a fixed L/D exposed two different linear shear flows; one from 0.0 to 2.0 feet per second and one from 0.0 to 4.0 feet per second. Both cases have the same shear fraction, (i.e. 100%) and both have the same β, (i.e. D/L). Both cases need an additional dynamics parameter, such as the number of potentially excited modes, N_s, to indicate the likely participation of modes in the response.

Given that neither parameter describe the necessary dynamic properties of the cable, then the one to be preferred is $\Delta V/V_{MAX}$, because it most clearly defines the properties of the shear, without confusing the matter by introducing L/D.

HYDRODYNAMIC DAMPING IS CRITICAL IN DETERMINING DYNAMIC BEHAVIOR

The structural damping for tensioned marine structures susceptible to flow-induced vibration is usually very small and for structures in water is rarely the deciding factor in the determination of whether or not lock-in occurs. However, when lock-in does not occur or occurs over only a portion of the structure then hydrodynamic sources of damping can be large and become very important in determining dynamic response behavior. Whether or not a cable responds dynamically as if it is of infinite length or is dominated by standing waves depends heavily on hydrodynamic sources of damping.

How Long Is Long?

The Green's function of a cable is the response of the cable

to a unit harmonic exciting force at a specified location. Figure 11 shows the magnitude squared of the Green's function of a constant tension cable of length L to a unit harmonic force applied at its center. Figure 11B shows the response when the excitation frequency is equal to the natural frequency of the 5th mode and the damping ratio is 1% of critical damping. The response shown is dominated by the standing wave mode shape for the 5th mode. Single mode resonant response dominates this case. A single mode approximation to the total response would be adequate. In Figure 11C the excitation frequency is equal to the 99th natural frequency and the damping ratio is 10%. The Green's function reveals that the vibration never reaches the cable ends. This is an example of infinite cable behavior. In Figure 11D the natural frequency of the 9th mode is equal to the excitation frequency and the damping ratio is again 10%. In this case the Green's function reveals intermediate dynamic behavior. Some attenuation of the response exists between the point of excitation and the ends of the cable. Some standing wave behavior is also exhibited.

A very simple dimensionless parameter may be used to predict which type of response is to be expected. A general definition is given by $2L\zeta/\lambda$, where ζ is the damping ratio at the frequency of interest and L/λ is the ratio of the cylinder length to the average wavelength. Average wavelength is used to accommodate modest variations in tension. The reason that this parameter is the relevant one is that for linear damping, the rate of decay of an harmonic wave travelling on a cable or beam is given by:

$$\text{spatial attenuation} = e^{-\zeta kx} = e^{-2\pi\zeta x/\lambda} \qquad (9)$$

Hence, a wave travelling one length of the cable would decay by the factor $e^{-2\pi\zeta L/\lambda}$. If the exponent $-2\pi\zeta L/\lambda$ is large, then the attenuation is also large and the response of the system will be like that of an infinite cable. When the exponent is small, little attenuation occurs, the exponential approaches 1.0 and standing wave resonant response would be typical. For the special cases of

uniform cables and beams with pinned ends and constant tension, the factor $2L/\lambda$ equals the mode number, n. and the parameter $2\zeta L/\lambda$ reduces to $n\zeta_n$. This is simply the product of the mode number and the damping ratio for that mode. In Figures 11 B, C, and D this parameter varies from 0.05 (standing wave with no apparent spatial attenuation) to 0.9 (strongly attenuated standing wave) to 9.9 (infinite cable response).

A recommended guide for interpreting the parameter $2\zeta L/\lambda$ or $n\zeta_n$ is as follows. When it is less that 0.2, clear standing wave behavior is to be expected over the entire cylinder. However, more than one mode may be present in the response. When it is greater than 2.0, then infinite cable behavior is the dominant characteristic. Between 0.2 and 2.0 this parameter implies that at the frequency of interest spatial attenuation will be important, but reflection from the ends will create a periodic modulation in the observed response of the cable, like that in Figure 11D.

The terminations of cylinders which exhibit infinite cable characteristics deserve a special note. At the ends reflections do occur, causing a local standing wave like pattern, which attenuates rapidly with distance from the end.

The problem for the designer is to estimate both the mode number, n, and the damping ratio, ζ_n. The mode number or its equivalent, twice the length to wavelength ratio, is relatively easy to obtain. The damping ratio, however, is not so obvious. Does one use structural damping or does one include the hydrodynamic sources of damping? This was a very controversial point in the mid to late 1970's. Ultimately most researchers, including the author, agreed that the structural non-hydrodynamic sources were the only important ones. When considering response in sheared flows that conclusion is completely false. The flaw is that in the 1970's the reasoning was narrowly focused on lock-in. Shear flow phenomena were not being seriously considered. Lock-in over the entire structure was the focus of most discussions. Under pure lock-in conditions the damping, which must be considered when evaluating the reduced damping parameter, is the structural damping. Under

unusual conditions lock-in may occur but not over the entire structure. In these cases hydrodynamic damping from the nonlock-in regions should be included in the damping, when computing the reduced damping.

Under nonlock-in conditions in sheared flow hydrodynamic damping must be considered, as it is often many times greater than the structural damping. This will be discussed in the next section.

Hydrodynamic Damping Estimation

A detailed hydrodynamic damping model is presented in Vandiver and Chung, 1987[15]. A simplified model, adequate for many applications is presented here. At any specific location an instantaneous drag force per unit length may be defined as the force in the direction of the instantaneous relative fluid flow, as shown in Figure 12. The fluid velocity relative to the cable is the vector sum of the free stream velocity V(x) and the negative of the local cross-flow cable velocity $\dot{y}(x,t)$. The in-line cable velocity $\dot{z}(x,t)$ is assumed small and is neglected (it could be included if greater precision was desired). If one assumes the drag force to be proportional to the relative velocity squared, then the magnitude of the drag force takes the form given below.

$$F_D(x,t) = \tfrac{1}{2}\rho_f C_D \cdot D \cdot \{V^2 + \dot{y}^2\} \qquad (10)$$

Letting, $B = \tfrac{1}{2}\rho_f C_D \cdot D$, the component of the drag force in the y or cross flow direction is by simple trigonometry given by:

$$F_y(x,t) = -B \cdot \dot{y}\{V^2+\dot{y}^2\}^{\frac{1}{2}} \qquad (11)$$

The damping force in equation (11) is a non-linear function of $\dot{y}$. It is helpful to find a linear equivalent damping constant r(x) which dissipates the same energy per cycle as the non-linear one. This is the approach carried out explicitly in Vandiver and Chung, 1987 [15]. However, under many conditions the following simplifi-

cation is quite acceptable. When $V(x)^2 >> \dot{y}^2$, then the cross flow damping force per unit length reduces to:

$$F_y(x,t) = B \cdot V(x) \cdot \dot{y} = r(x) \cdot \dot{y} \qquad (12)$$

where $r(x) = \frac{1}{2}\rho_f C_D D \cdot V(x)$

This is a simple linear damping model. The local damping ratio is then given by:

$$\zeta = r(x)/[2\omega_v(m+\rho_f \pi D^2 C_a/4)] \qquad (13)$$

Substituting in for r(x) yields

$$\zeta = \frac{1}{2}\rho_f C_D D \cdot V(x)/[2\omega_v(m+\rho_f \pi D^2 C_a/4)] \qquad (14)$$

The local velocity can be expressed in terms of reduced velocity and the local shedding frequency as follows:

$$V(x) = D \cdot \omega_s V_R/2\pi \qquad (15)$$

Taking the example that the fluid is water, then the hydrodynamic damping ratio may be expressed as

$$\zeta_h = C_D V_R \omega_s(x)/[2\pi^2 \omega_v(s.g.+C_a)] \qquad (16)$$

Strictly speaking, this is the local damping ratio for an infinite length cylinder. However, by using the techniques of modal analysis, as shown in [15], one may compute the modal damping ratio for a specific mode n. In order to do this one must specify the shear profile. In the case of a linear shear profile the modal hydrodynamic damping ratio is given for mode n by:

$$\zeta_{h,n} = C_D V_R \omega_{s,max}/[4\pi^2 \omega_n(s.g.+C_a)] \qquad (17)$$

Where $\omega_{s,max}$ is the maximum shedding frequency, corresponding to the peak flow velocity , and ω_n is the natural frequency of mode n.

In the above two equations V_R was introduced so as to allow the local flow velocity to be expressed in terms of the local shedding frequency $\omega_s(x)$. Therefore, V_R should be taken to have a value of about 5.9, which is the average value observed in the field. This value, 5.9, is a refinement on the value of 5.0 given previously in references [15] and [16].

These damping models were verified in a field experiment which is discussed in the next section of this paper. Prior to that discussion, it is important to consider one refinement of the modal damping model given in equation (17). Each excited mode will have a region of the cable where the local vortex shedding frequency and the natural frequency coincide as depicted in Figure 13. In this region net power flows into that particular mode[15]. This region should be excluded in the calculation of hydrodynamic damping for that particular mode. This would cause a corresponding reduction in the damping ratio predicted by Equation 17.

The precise delineation of these power in and damping exclusion ranges, is at the present rather uncertain. It is discussed in Brooks 1987 [1], Wang et al, 1985 [19], and Vandiver and Chung, 1987 [15]. The spatial extent of the damping exclusion region for each mode will decrease as the number of responding modes, N_s, increases. When N_s exceeds approximately 10, the magnitude of the correction to the estimated modal damping ratio, becomes sufficiently small that one need not bother with it.

The assumption that $V(x)^2 >> \dot{y}^2$ is not valid in the slow part of a stratified flow in which vibration from a high velocity region passes suddenly into a region of very low or zero flow velocity. In the case of a region of zero flow a different approximation may be used, such as discussed by Sarpkaya,1979 [10].

A verification of the importance of hydrodynamic damping in sheared conditions was accomplished in a field experiment conducted in the summer of 1986, and reported on below.

THE SHEARED FLOW EXPERIMENTS AT LAWRENCE, 1986

The experiments were conducted for the purpose of validating the hydrodynamic damping model, and obtaining experimental data for the case that $n\zeta_n$ fell between the extremes of lightly damped individual modes, typical of the cables at Castine, and infinite cable behavior typical of the cables tested in St. Croix. At Castine in 1981, fourth mode lockin vibration of the cable or pipe resulted in $n\zeta n$ values of 0.008 and 0.004 respectively. Standing waves with no apparent attenuation were observed. For the St. Croix experiments the total damping was approximately 1.5% and a typical value of $2\zeta L/\lambda$ was 2.3 at a length of 950 ft. Infinite cable behavior was observed.

The experiments were conducted during the summer of 1986. A complete description, including many figures, may be found in references [2,15,16]. The test site was a mill canal, built in 1848 in Lawrence, Massachusetts. A dam diverts the water from the Merrimack River into the canal. The flow is controlled by four submerged gates, which are spaced at equal horizontal intervals beneath a gate house at the head of the canal. By controlling the various gate openings a sheared flow can be developed horizontally across the width of the canal, which is approximately 58 feet. The average depth of the canal is ten feet.

The test cable location was approximately 250 feet downstream of the gate house. The cable was tensioned horizontally across the width of the canal about one foot under the surface, as shown in Figure 14. Heavy steel pipe supports transferred the cable loads to the walls of the canal. Tension was applied to the cable via a system of pulleys and a hand-operated winch. For a given winch position the cable had essentially constant arc length. The tension then varied slowly with mean drag force on the cable. Tension was measured with a tension cell connected in series between the cable and winch.

Five feet upstream of the test cable, a simple traversing mechanism was suspended from a taut wire above the waters of the canal to carry a Neil Brown Instruments DRCM-2, two-axis acoustic

current meter. The transducer was located about one foot under water and was oriented so that the instantaneous velocity was resolved into two components in the horizontal plane. The velocity was measured at two samples per second.

The 58-foot long test cable is shown in Figure 15. It consisted of a 1.125 inch rubber hose with a 0.5 inch inside diameter. Seven 0.16 inch diameter braided kevlar cables were carried inside of the hose. Each kevlar cable had seven conductors inside of it. Three kevlar cables were used solely as load carrying members, three cables were used to carry accelerometer signals and power, and one cable was used as a spare.

Six biaxial pairs of force balance accelerometers were placed on the centerline of the cable at locations shown in the figure. Each biaxial pair was 0.5 inches in diameter and 3 inches long. Space was created for the kevlar cables to pass around the accelerometers at these locations, with no change in the outside diameter of the hose. The accelerometers, tension cell, and current meter were the same as used in previous experiments conducted at Castine, Maine.

The 12 accelerometer outputs, tension, and current data were carried via a multi-conductor cable from the test cable to the gatehouse, where a Digital Equipment MINC-23 data acquisition computer was located. Fourteen data channels were digitized and stored on floppy disks.

Sheared Current Profiles

The current profiles were measured prior to response tests. The results of three different profiles are shown in Figure 16. They are designated shear flow profile 1, 2, and 3 (SFP1, etc.). SFP3 was the steepest shear with a peak flow velocity at times exceeding 4 feet per second and a minimum flow velocity of -0.5 feet per second. The minus indicates reverse flow. SFP2, a milder shear, ranged from 2 feet per second down to zero in a nearly linear profile. SFP1 was made as close to uniform as possible by careful positioning of the gates. The velocity varied approximate-

ly 30% along the length.

For all profiles the flow was highly turbulent. The turbulence intensity level was from 10 to 20 percent of the maximum current in the profile. The longest time scale of the turbulence was up to several seconds in length, and was associated with large eddies, which were carried downstream from the gatehouse.

An important observation is that the turbulence was able to prevent constant amplitude, single mode lock-in from occurring, even with the most uniform profile, SFP1, which had a $\Delta V/V_{MAX} = 0.3$.

PREDICTED AND MEASURED HYDRODYNAMIC DAMPING

The structural damping measured by free vibration decay tests in air for the test cable in this experiment was about 0.3% of critical for the frequency ranges and tensions later experienced in the water. A more precise measure is not important because the hydrodynamic damping will be shown to be far larger.

Figure 17 is a sample time history of the response of the test cable in the highly sheared flow, for which $\Delta V/V_{MAX}$ was 1.125. Simultaneous time histories of cross-flow acceleration are given for all six measurement locations. It is quite obvious that the high velocity locations had higher response than the low velocity regions. In this case the rms displacement was 0.3 diameters at x=13L/16 and 0.5 diameters at x=L/8. The tension was 151 pounds and the natural modes were 0.6 Hz apart. The peak vortex shedding frequency corresponded to about the 10th natural frequency, and therefore N_s the number of excited modes was approximately 10. Enough modes were involved in the response that variation in mode shape is not a particularly important factor when comparing the rms response of one location to another.

The decrease in observed rms response level between positions near opposite ends of the cable was only possible if $n\zeta_n$ was greater than 0.2. Structural damping alone with a value of $\zeta_s = 0.003$, leads to an estimate of $n\zeta_n$ for the 10th mode of 0.03; too small to explain the spatial attenuation. Hydrodynamic damping was impor-

tant in this case and can be estimated using equation 15.

For this experiment the specific gravity of the cable was 1.34. Letting the average added mass coefficient, C_a, and the drag coefficient, C_D, both equal 1.0, and setting V_R to a value of 5.9 leads to the following prediction for hydrodynamic modal damping ratios.

$$\zeta_{h,n} = 0.064\omega_{s,max}/\omega_n \tag{18}$$

The ratio $\omega_{s,max}/\omega_s$ is approximately one for the highest excited mode, independent of mode number. Therefore, for the highest excited mode the hydrodynamic modal damping ratio is predicted to be 6.4%, which when added to the structural damping ratio yields a total damping of 6.7%. Since this was mode ten, then the parameter $n\zeta_n$ is .67. For the lower excited modes the hydrodynamic damping ratio is larger than 6.4% and increases in proportion to the ratio $\omega_{s,max}/\omega_s$. However, since n is smaller for lower modes, one finds that $n\zeta_n$ remains constant at 0.67. This value is as expected between the limits of 0.2 and 2.0 and consistent with the observed spatial attenuation in response.

To conclusively demonstrate that the predicted hydrodynamic damping is correct, one must use it in a prediction model, which includes the effects of current shear and hydrodynamic damping. Such a model is proposed and used in Chung, 1987 [2], and Vandiver and Chung, 1988 [16]. Comparisons between measured and predicted response for the shear flow experiments at Lawrence are presented. One example is given here.

Figure 18 is a comparison between the predicted and measured acceleration response spectrum of the cable at x = 13L/16. The cable was exposed to the intermediate shear profile (SFP2). The predictive model includes the effects of shear, turbulence, hydrodynamic damping, correlation length, and higher order harmonics of the vortex shedding frequencies. For this case the maximum flow velocity was approximately 2.0 ft/s and the highest excited mode was the fifth, with a predicted value of total damping of 6.7%.

Again $n\zeta_n$ is constant and independent of mode number with a value of 0.33. The number of excited modes was 5 and $\Delta V/V_{max}$ was 100%. Lock-in was not observed. The controlling green's functions for the cable had characteristics similar to those shown in Figure 11D and were consistent with values of $n\zeta_n$ equal to 0.3.

In summary, the Lawrence experiment provided an excellent opportunity to test the validity of using the dimensionless parameters recommended in this paper for predicting response characteristics. These parameters were N_s, $\Delta V/V_{max}$, and $n\zeta_n$, where ζ_n included hydrodynamic effects.

The Lawrence tests also provided an opportunity to conduct a simple direct comparison between predicted and observed infinite cable hydrodynamic damping, as discussed next.

Impulse Response Under High Tension in a Turbulent Uniform Flow

With large hydrodynamic damping the vibration excited at one location is attenuated as it travels through the cable to distant points. This was confirmed by an independent measurement. Under steady state flow-induced vibration conditions, the cable was struck impulsively with a wooden pole, at a location near one end. An impulse propagated through the cable. Figure 19 shows the simultaneous time histories at all six accelerometer locations. The impulse can be seen to travel from one location to the next with a travel time delay and an attenuation due to damping. By comparing the spectra of the accelerometer time histories it is possible to estimate the frequency content of the impulse and the effective damping coefficient. The cable tension was 450 pounds, the current was the approximately uniform profile (SFP1), $\Delta V/V_{max}$ = 0.3. The cable's flow-induced vibration response was dominated by nonlock-in third mode response at a natural frequency of 3.0 Hz and an rms response of approximately 1/2 diameter. The predicted damping experienced by the impulse as it travelled along the cable may be obtained using the damping model for waves travelling along an infinite cable. The infinite cable model is valid for the period of time prior to the reflection of the pulse from the far

end of the cable. Using equation (16) and the following values for the necessary constants, the hydrodynamic damping prediction is obtained. Letting C_D = 2.0, V_R = 5.9, C_a = 1.0, and s.g. = 1.34, yields:

$$\zeta_h = .256\omega_s(x)/\omega_v \tag{19}$$

The dominant shedding frequency was 3.0 Hz. The impulse had most of its energy in the 15 to 24 Hz range. Taking 18 Hz as a frequency typical of the impulse, the above equation yields a hydrodynamic damping prediction of 4.3%. A C_D of 2.0 was used to reflect the relatively larger rms response (0.5 diameter).

If the damping behaves linearly, then the attenuation of a wave amplitude as a function of distance travelled is given by:

$$\text{attenuation} = e^{-\zeta kd} = e^{-\zeta\omega d/c} \tag{20}$$

where k = ω/c, the wave number

c = speed of wave propagation

d = distance travelled

Since response spectra are proportional to response amplitude squared, then the attenuation of the impulse energy in the 15 to 24 Hz band should be given by the square of the above equation. If A_1 and A_2 are the spectral magnitudes in the 15 to 24 Hz band for two different locations, a distance d apart, then the effective damping may be deduced as in the following equation.

$$\zeta = c\cdot\ln(A_2/A_1)/2\omega_v d \tag{21}$$

The two spectra in Figure 21 are used here as an example. The locations were separated by 19.3 feet. Choosing a typical frequency of f=18 Hz, and noting that $\omega = 2\pi f$, d = 19.3 feet, C = 120 feet/sec, and the ratio of the two spectra in the 15 to 24 Hz band is approximately six to one, results in an estimate of ζ = 0.049 or 4.9% compared to the prediction of 4.6%. Many similar calculations were performed between different locations and for different impulse events. The results fell into a range of 4 to 6% total

damping.

If one substitutes the formula for damping as given in equation 19 into equation 20 for wave attenuation, the result is independent of vibration frequency. This is consistent with the expression for damping ratio in equation (16), which states that damping ratio decreases with frequency. Over a fixed distance, d, high frequency waves travel more wavelengths than low frequency waves, which have greater damping but travel fewer wavelengths. Over a fixed distance all vibration frequency components attenuate the same amount.

SUMMARY AND CONCLUSIONS

The design of moorings, ROV tethers, pipelines, and petroleum drilling and production risers all depend on the expected magnitude and frequency of vortex-induced vibration. Lock-in usually results in the largest amplitudes of vibration and the largest mean drag coefficients, and, therefore is considered in most situations to be the worst case. Establishing whether or not it will occur is usually of great concern. This paper has attempted to reveal those parameters which have greatest influence over the occurrence of lock-in for flexible cylinders with large L/D, and has provided case studies to support the conclusions.

The parameters most useful for determining whether or not lock-in will occur are the shear fraction, $\Delta V/V_{max}$, and the number of potentially excited modes, N_s, and to a usually lesser extent the turbulence intensity.

When lock-in is likely to occur, the mass ratio has a strong effect on determining the range of reduced velocity over which lock-in can occur. If this range is narrow, then lock-in may occur only for narrow bands of flow velocity. For low mass ratio cylinders the reduced velocity lock-in range is broad and lock-in regions may overlap, such that transition from lock-in in one mode to the next is possible as the velocity increases.

Under lock-in conditions the response amplitude may be predicted using the response parameter, S_g, based on the structural

damping. However, S_c has been shown not to be a function of mass ratio as commonly believed.

When multiple modes respond under nonlock-in conditions, then another parameter $n\zeta_n$, has been shown to reveal whether wave propagation or standing wave characteristics dominate the nature of the dynamic response. In sheared flows which create nonlock-in dynamic response, hydrodynamic damping has been shown to be usually much more important than structural damping in governing response amplitude.

Many conclusions require further refinement, largely through experimental work. In many cases the critical parameters are known, but the values which mark the transition from one type of behavior to another need refinement. For example, what combination of values of N_s, the number of potential responding modes, and $\Delta V/V_{MAX}$, the shear fraction, define the boundary between lock-in and non-lockin. These and many other similar problems require experimental data before they can be resolved.

ACKNOWLEDGEMENTS

This research was supported by a consortium of government and industry sponsors. These sponsors included: Amoco, Chevron, Conoco, Exxon Production Research, Mobil, Petrobras, Shell Development Co., the Technology Assessment and Research Program of the Minerals Management Service, and the MIT Sea Grant Program under agreement number NA86AA-D-SG089.

REFERENCES

1. Brooks, I.H., "A Pragmatic Approach to Vortex-Induced Vibrations of a Drilling Riser", Proc. 1987 Offshore Technology Conference, OTC 5522, Houston, May 1987.

2. Chung, T. Y., "Vortex-Induced Vibration of Flexible Cylinders in Sheared Flows", Ph. D. dissertation, MIT Dept. of Ocean Engineering, May, 1987.

3. Chung, T. Y., "Vortex-Induced Vibration of Flexible Cylinders Having Different Mass Ratios", Report No. UCE 440-1283ED, Korea Research Institute of Ships and Ocean Engineering, Dec. 1989.

4. Griffin, O. M. & Ramberg, S. E., "Some Recent Studies of Vortex Shedding With Applications to Marine Tubulars and Risers", J. of Energy Resources Technology, Vol. 104, March 1982.

5. Griffin, O. M., "The Effects of Current Shear on Vortex Shedding", Proc. Separated Flow Around Marine Structures, Norwegian Inst. Of Technology, Trondheim, 1985.

6. Griffin, O.M. and Vandiver J.K., "Vortex-Induced Strumming Vibrations of Marine Cables with Attached Masses", Journal of Energy Resources Technology, Vol. 106, Dec. 1984.

7. Kim, Y.H., Vandiver, J.K. and Holler, R., "Vortex-Induced Vibration and Drag Coefficients of Long Cables Subjected to Sheared Flow", Proc. 4th OMAE Symposium , Volume One, ASME, Dallas, TX, Feb. 1985, J. of Energy Resources Technology, Vol. 108, March 1986.

8. Pham, Thai Q., "Evaluation of the Performance of Various Strumming Suppression Devices on Marine Cables", MIT Dept of Ocean Engineering Master's thesis, February 1977.

9. Sarpkaya, T., "Transverse Oscillations of a Circular Cylinder in Uniform Flow, Part I", Naval Postgraduate School Report No. NPS-69SL77071, July 1977.

10. Sarpkaya, T., "Vortex-Induced Oscillations: A Selective Review", Journal of Applied Mechanics, Vol. 46, June 1979.

11. Shargel, Robert, and Vandiver, J.K., "The Drag Coefficient for a Randomly Oscillating Cylinder in a Uniform Flow," M.I.T. Dept. of Ocean Engineering, December 1982

12. Stansby, P.K., "The Locking-on of Vortex Shedding Due to the Cross-stream Vibration of Circular Cylinders in Uniform and Shear Flows", J. Fluid Mechanics, Vol 74, part 4, pp. 641-665, 1976.

13. Vandiver, J.K., "Drag Coefficients of Long Flexible Cylinders," Proc. 1983 Offshore Technology Conference, OTC 4490, Houston, 1983.

14. Vandiver, J.K., "The Predictions of Lock-in Vibration on Flexible Cylinders in a Sheared Flow", Proc. 1985 Offshore Technology Conference, OTC 5006, May 1985, Houston, TX.

15. Vandiver, J.K., & Chung, T.Y., "Hydrodynamic Damping on Flexible Cylinders in Sheared Flow", Proc. 1987 Offshore Technology Conference, OTC 5524, Houston, May 1987.

16. Vandiver, J.K., & Chung, T.Y., "Predicted and Measured Response of Flexible Cylinders In Sheared Flow", ASME Winter Annual Meeting, Symposium on Vortex-Induced Vibration", Chicago, Dec. 1988.

17. Vandiver, J.K. and Jong, J.-Y., "The Relationship Between In-Line and Cross-Flow, Vortex-Induced, Vibration of Cylinders", J. of Fluids and Structures, Vol. 1, 1987.

18. Vandiver, J.K., and C.H. Mazel, "A Field Study of Vortex Excited Vibrations of Marine Cables," Proc. 1976 Offshore Technology Conference, Vol. I, OTC 2491, pp. 701-709, Houston, May 1976.

19. Wang, E., Whitney, D.K., and Nikkel, K.G., "Vortex Shedding Response of Long Cylindrical Structures in Shear Flow", Proc. 5th Intl. Symposium on Offshore Mechanics and Artic Engineering, Tokyo, April 1987.

20. Tashalis, D. T., "Vortex-Induced Vibrations of a Flexible Cylinder Near a Plane Boundary Exposed to Steady and Wave-Induced Currents", Journal of Energy Resources Technology, Vol. 106, June 1984.

21. Koch, S., Private Communication of Data from Experiments conducted in a towing tank by Exxon Production Research.

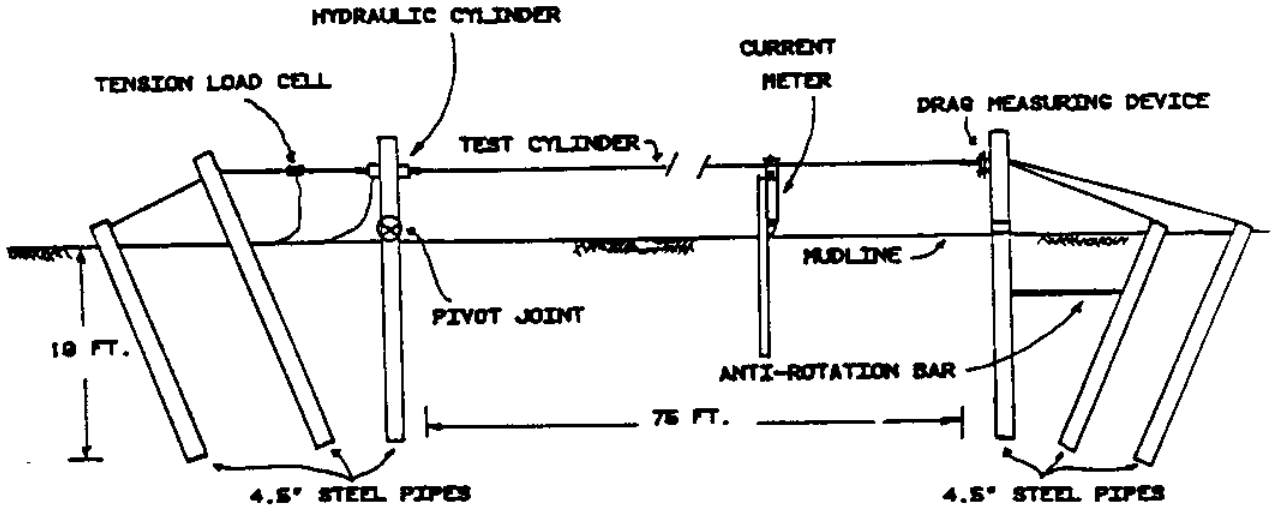

Figure 1. Castine Experimental Setup, 1981

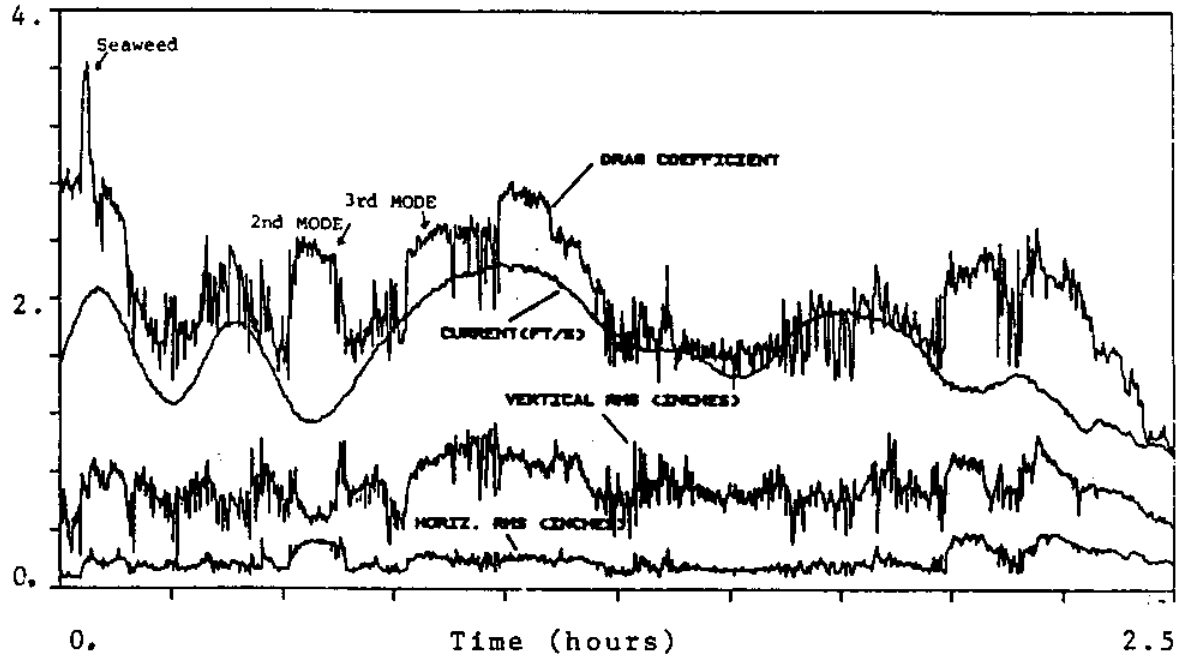

Figure 2. C_D, Current, RMS Displacement at L/6, for the Pipe at T = 670 - 920 LBS. C_D Error ± 10% at 2 ft/s, ± 15% at 1 ft/s.

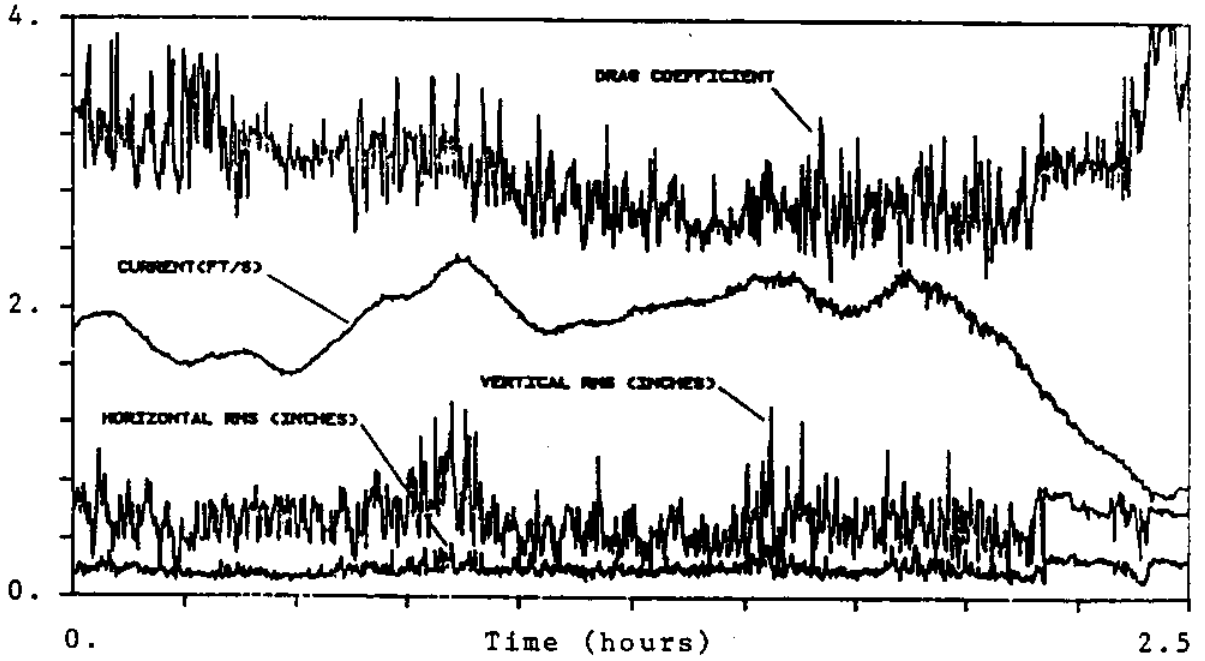

Figure 3. C_D, Current, RMS Displacement at L/6, for the Cable at T = 320 to 600 LBS. C_D + 0%, -20% Error Bound.

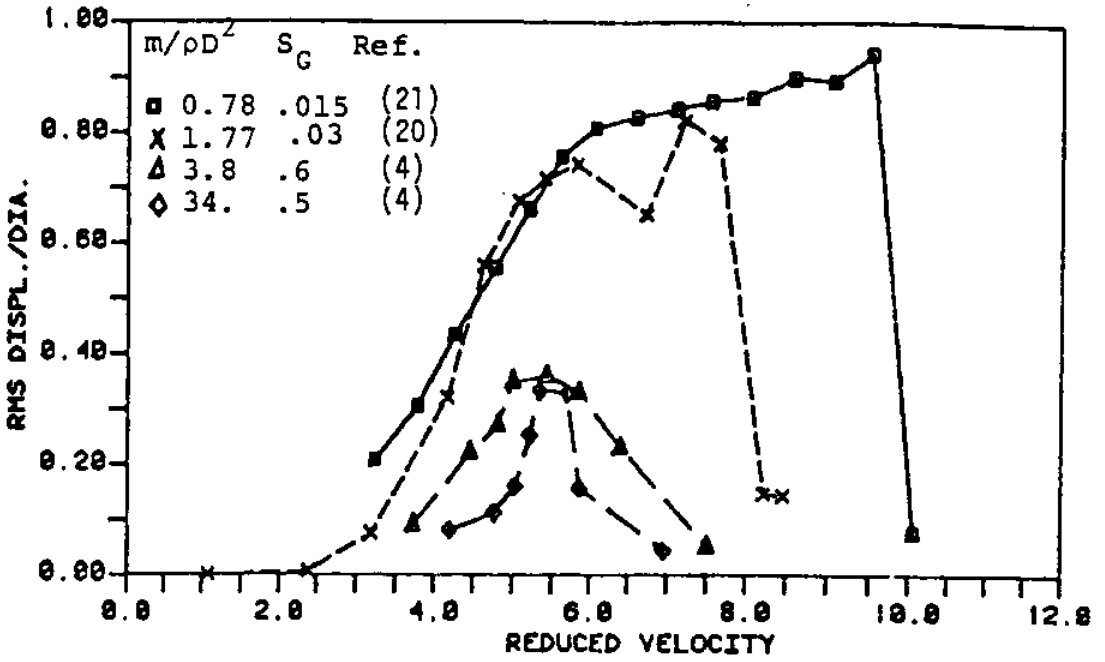

Figure 4. RMS Displacement versus Reduced Velocity for Various Mass Ratios; from [2].

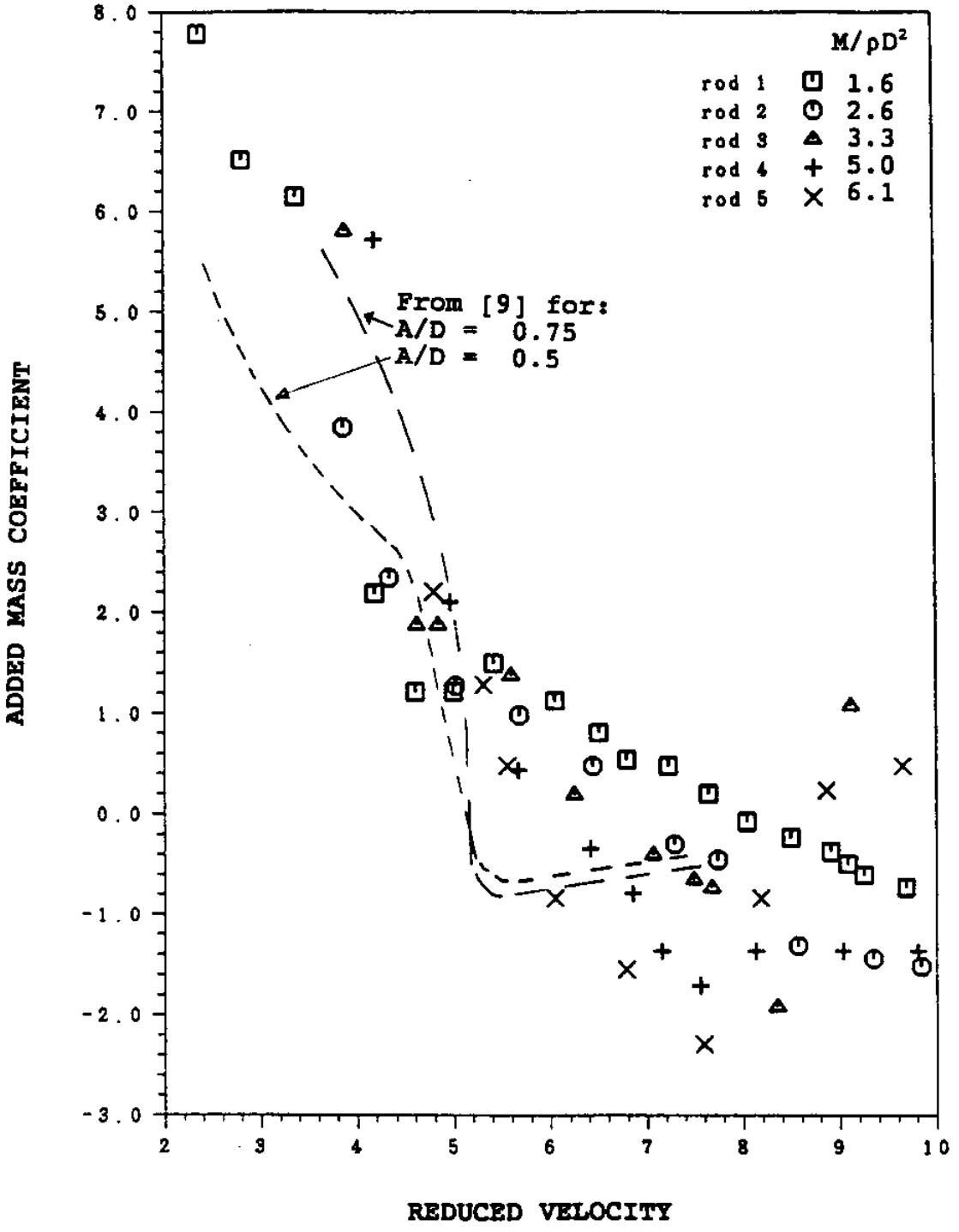

Figure 5. Effective Added Mass Coefficient Versus Reduced Velocity (from [3] & [9])

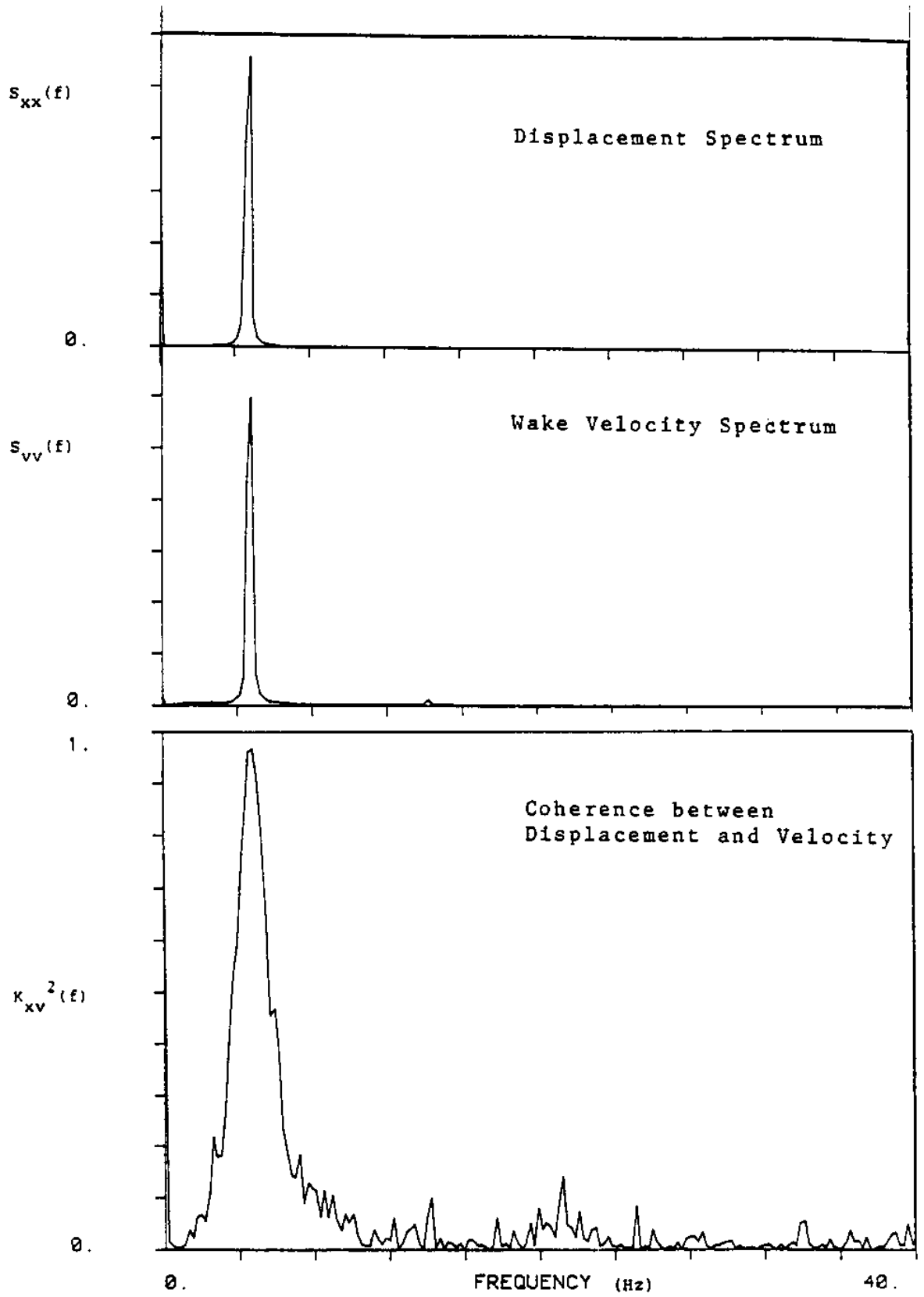

Figure 6. Displacement Spectrum, Wake Velocity Spectrum and Coherence for Sinusoidal Lockin Conditions: $R_e \approx 5000$, $A_{RMS}/D = .109$, from [9].

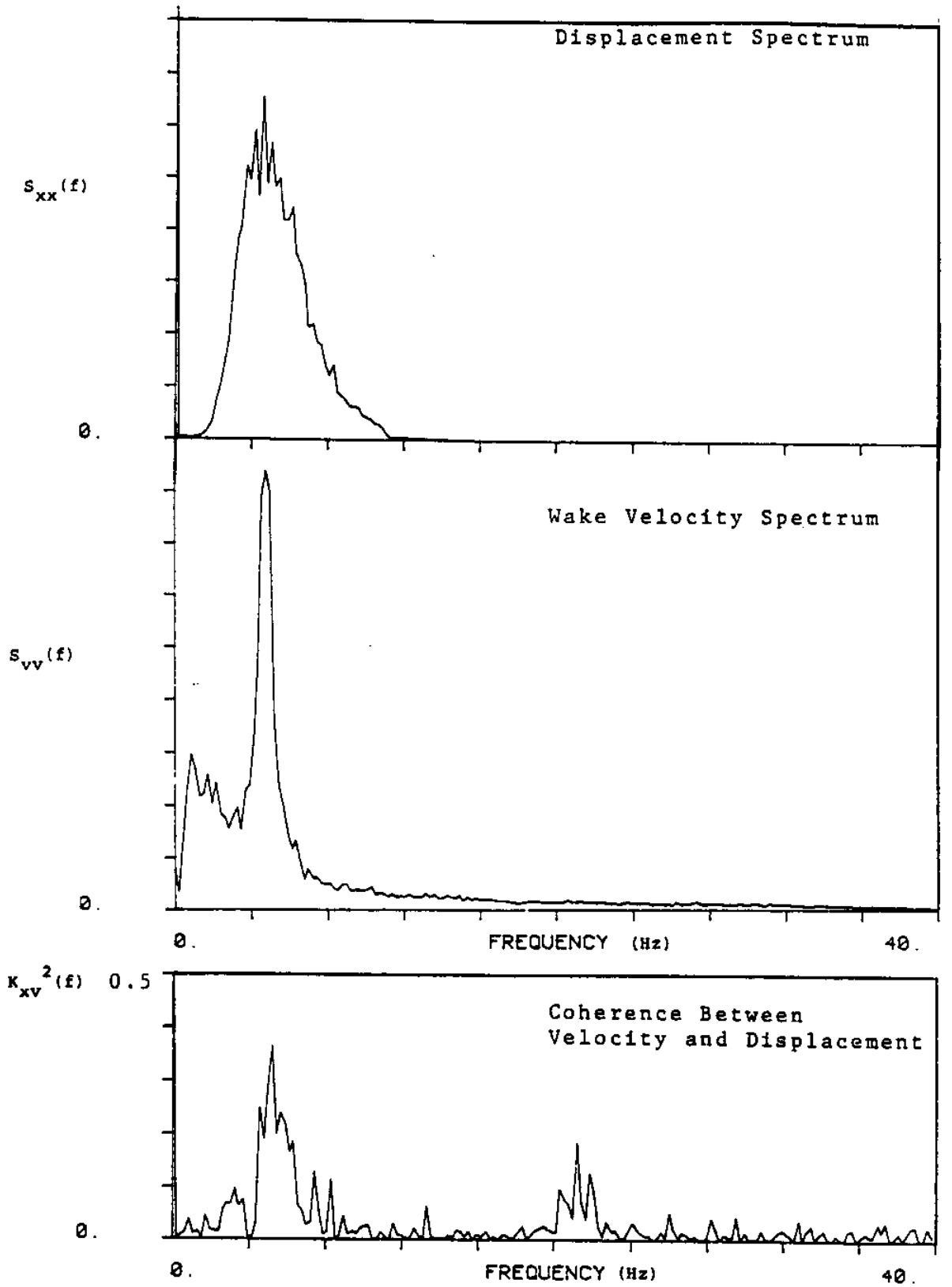

Figure 7. Displacement Spectrum, Wake Velocity Spectrum, and Coherence for Narrow Band Oscillations: $R_e \approx$, $A_{RMS}/D = .106$; from [9].

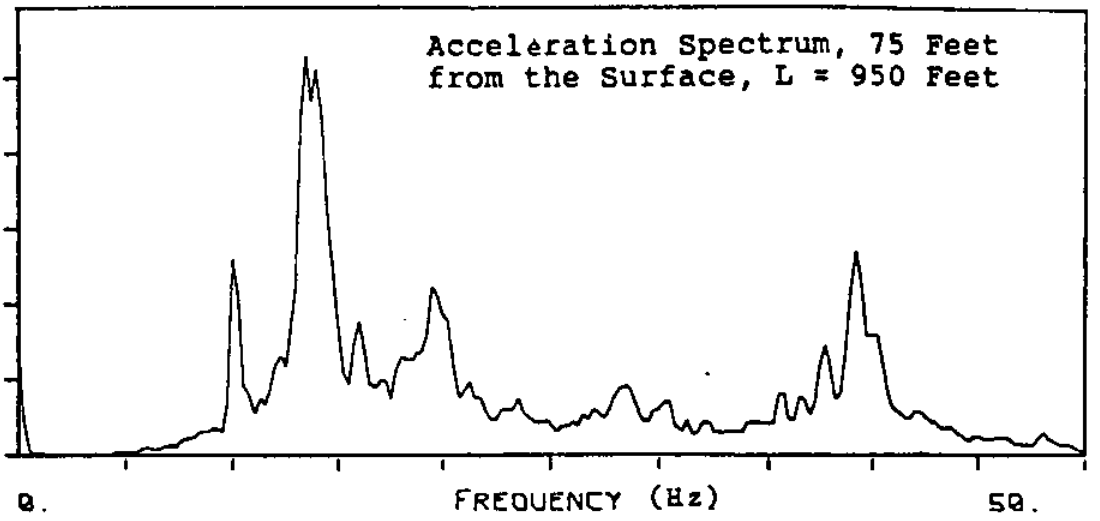

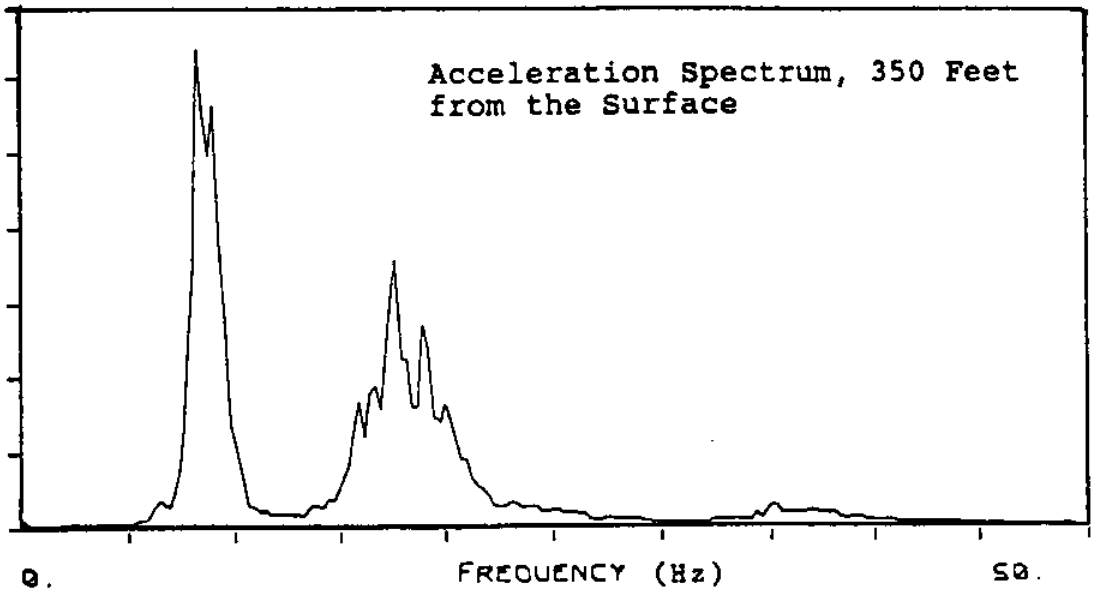

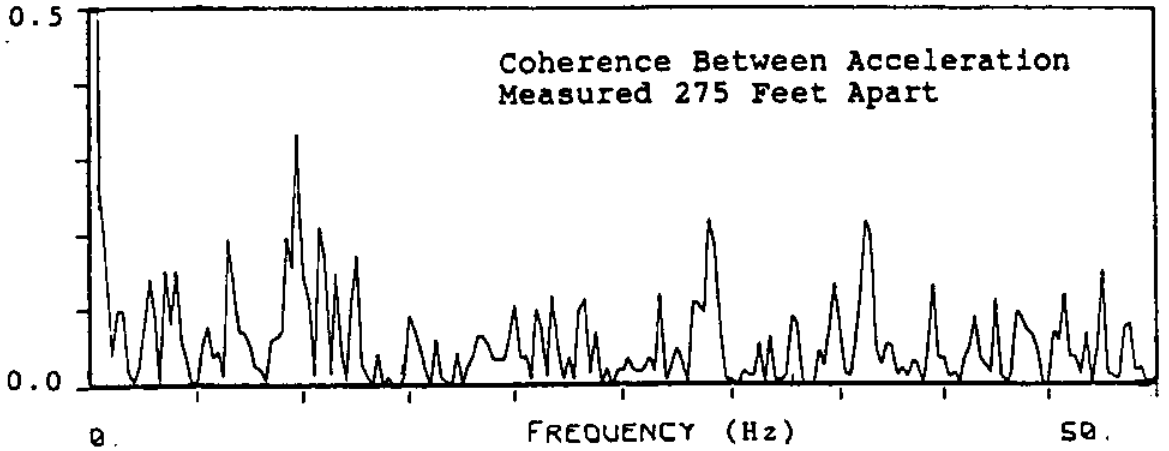

Figures 8, 9, 10. Acceleration spectra and Coherence for Two Locations Separated by 275 feet; St. Croix 1983 [6].

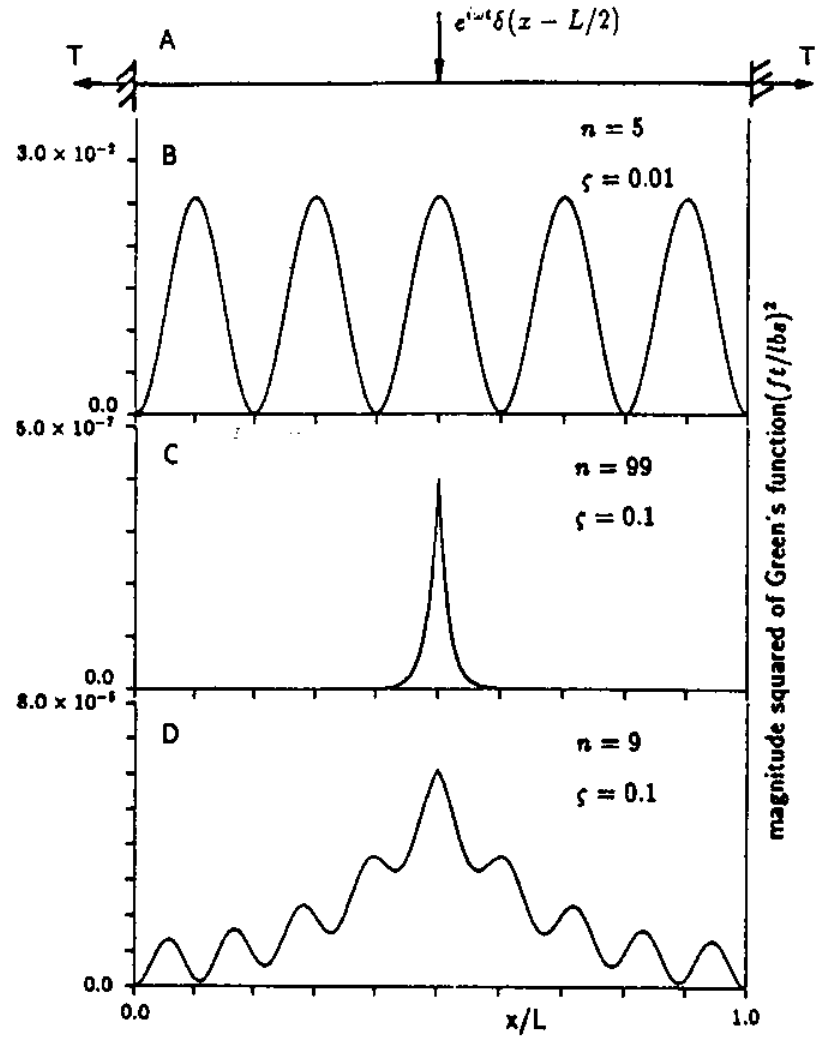

Figure 11. Magnitude of Response to a Unit Harmonic Force at L/2

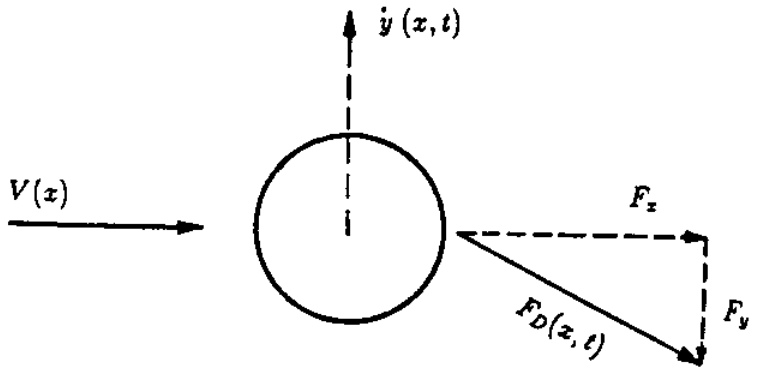

Figure 12. Damping Force Vector Components

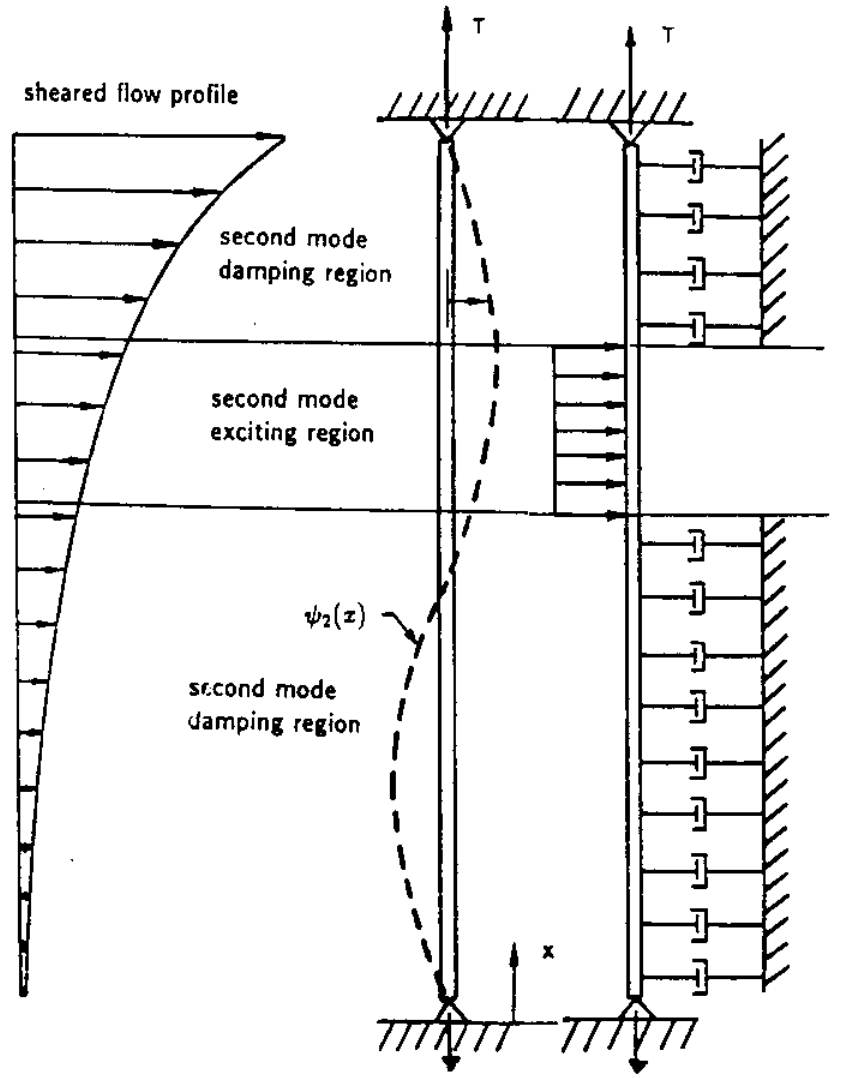

Figure 13. Power Flow Model for a Flexible Cylinder

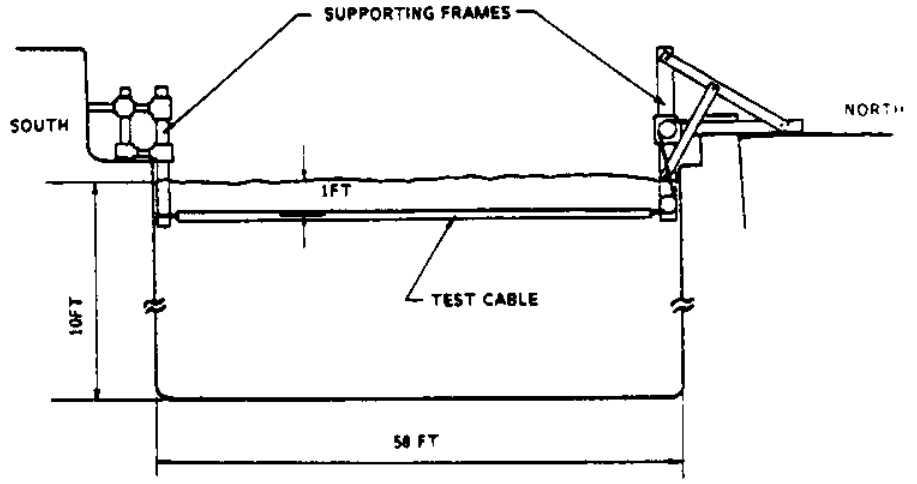

Figure 14. Lawrence Test Configuration, 1986

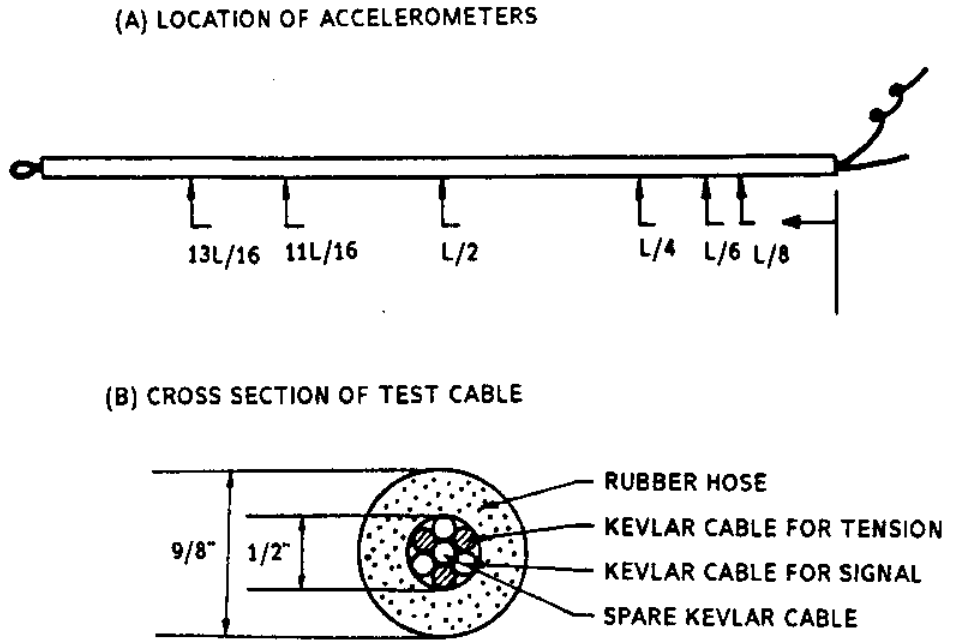

Figure 15. Lawrence Test Cable Construction

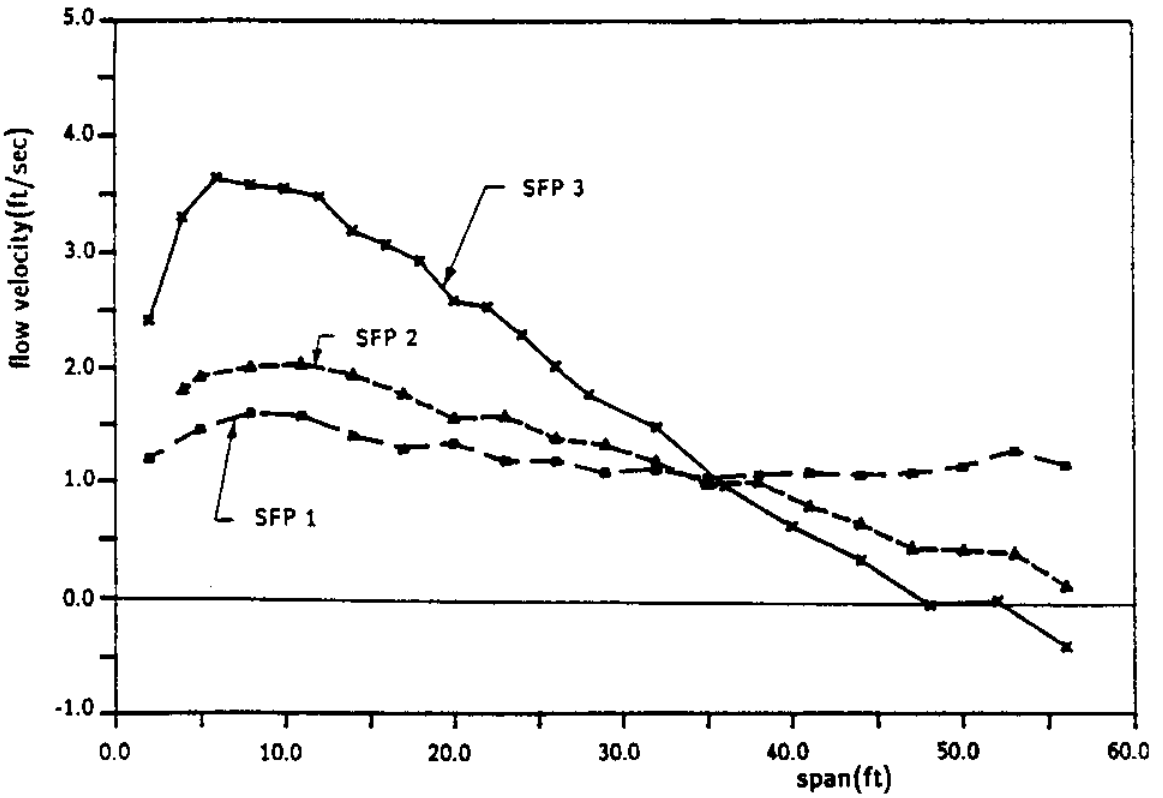

Figure 16. Shear Flow Profiles for the Lawrence Experiments

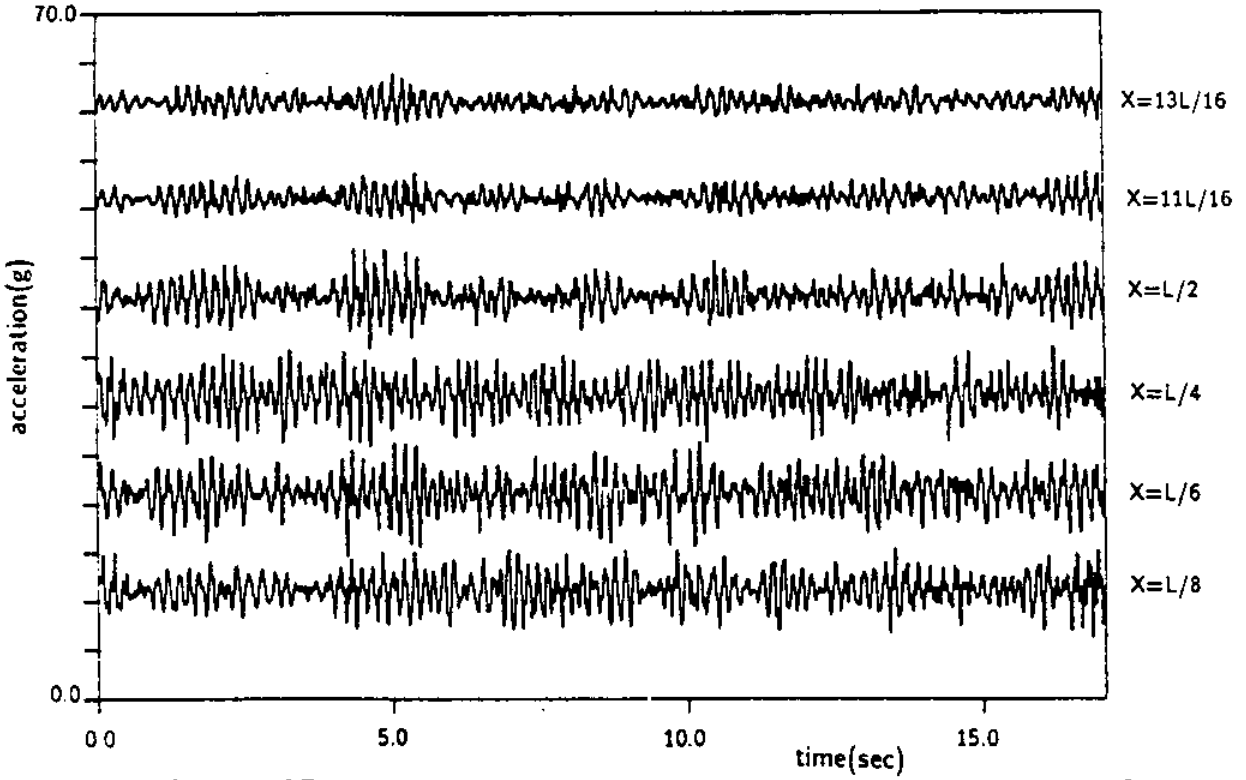

Figure 17. Cross-Flow Acceleration Time Histories for All Six Accelerometer Locations for the High Shear Case.

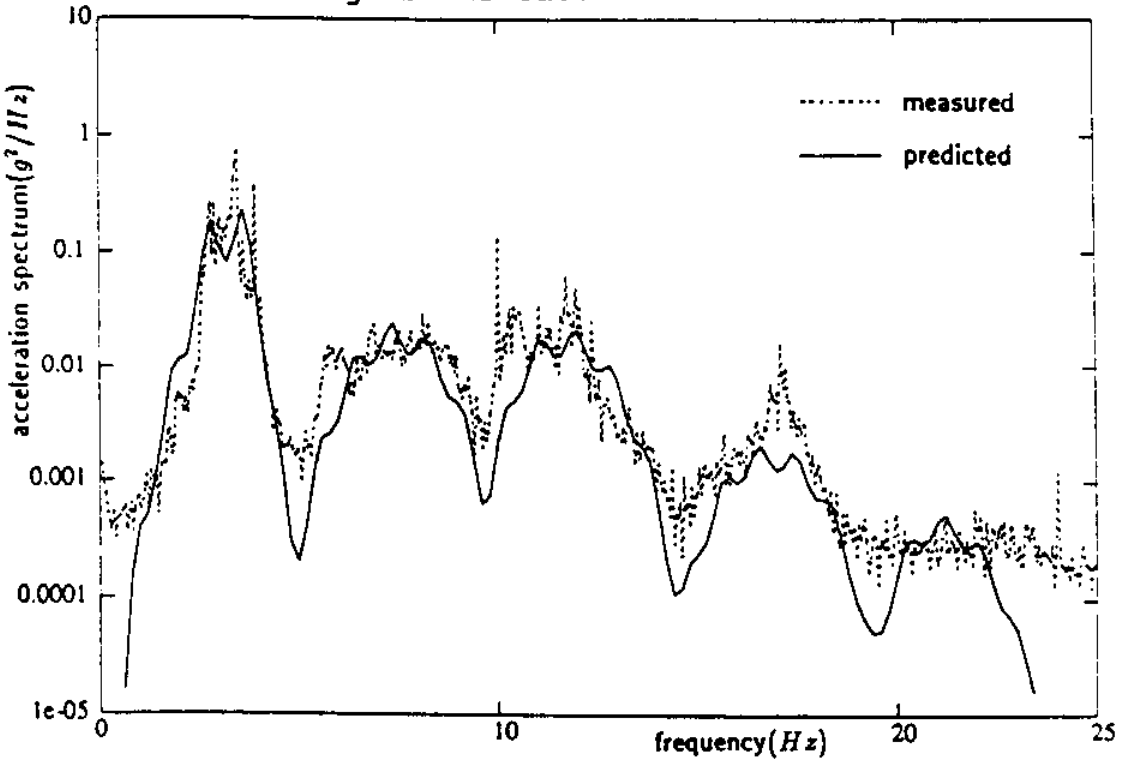

Figure 18. Measured and Predicted Acceleration Response Spectra at 13L/16 (Low Current Side) in SFP2.

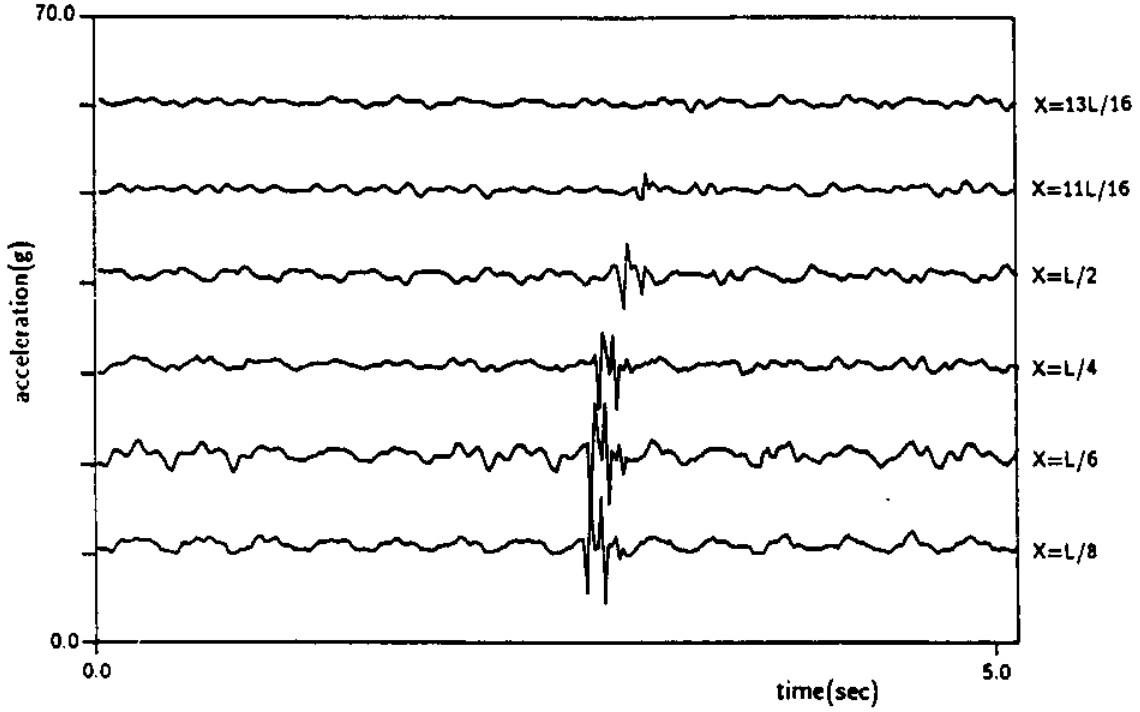

Figure 19. Measured Impulse Response Propagation Time Histories

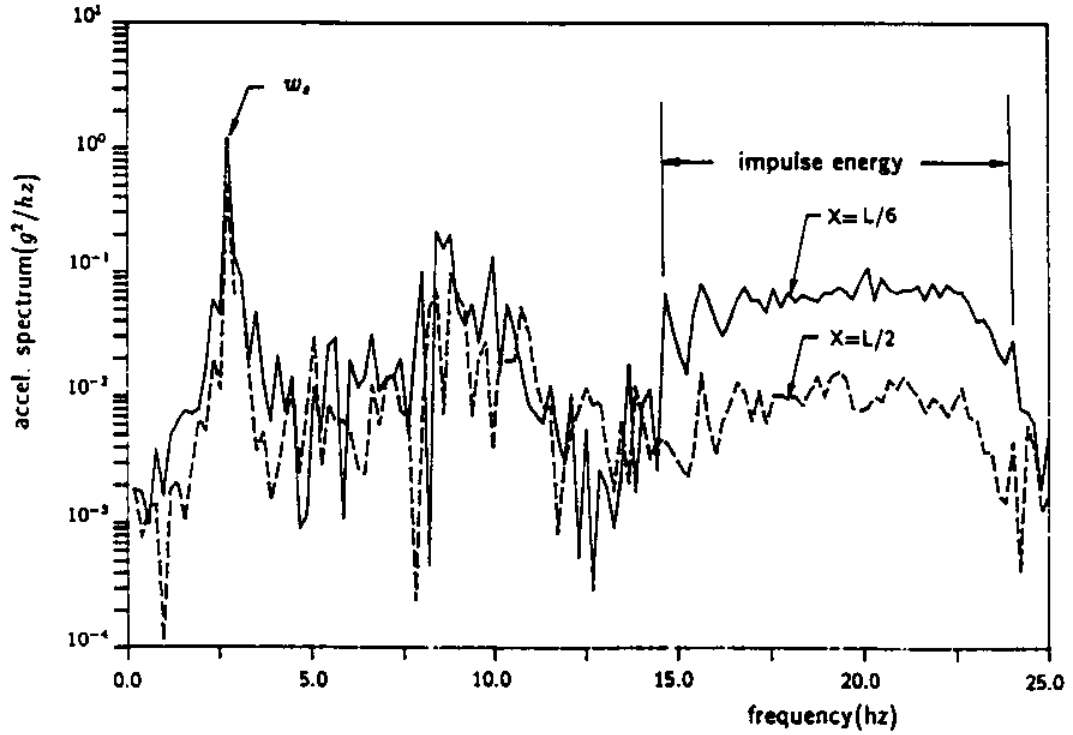

Figure 20. Measured Impulse Response Spectra at L/2 and L/6 in a Very Turbulent Uniform Flow